1-1-2012

Determining the Etiology of Decreased Tensile Strength in Tissues of Quarter Horses with Hereditary Regional Dermal Asthenia (HERDA)

Jacquelyn Elizabeth Bowser

Determining the etiology of decreased tensile strength in tissues of Quarter Horses with Hereditary Regional Dermal Asthenia (HERDA)

By

Jacquelyn Elizabeth Bowser

A Dissertation
Submitted to the Faculty of
Mississippi State University
in Partial Fulfillment of the Requirements
for the Degree of Doctor of Philosophy
in Veterinary Medical Science
College of Veterinary Medicine
Mississippi State, Mississippi

December 2012

Determining the etiology of decreased tensile strength in tissues of Quarter Horses with Hereditary Regional Dermal Asthenia (HERDA)

By

Jacquelyn Elizabeth Bowser

Approved:

Cyprianna E. Swiderski Associate Professor of Clinical Sciences (Major Professor)	Steven H. Elder Professor of Agriculture and Bioengineering (Committee Member)
Marzia Pasquali Committee Participant of Clinical Sciences (Committee Member)	Michael K. Brashier Associate Professor of Clinical Sciences (Committee Member)
Andrew J. Mackin Professor of Clinical Sciences (Graduate Coordinator)	Kent Hoblet Dean of the College of Veterinary Medicine

Name: Jacquelyn Elizabeth Bowser

Date of Degree: December 15, 2012

Institution: Mississippi State University

Major Field: Veterinary Medical Science

Major Professor: Dr. Cyprianna E. Swiderski, DVM, PhD, DACVIM

Title of Study: Determining the etiology of decreased tensile strength in tissues of Quarter Horses with Hereditary Regional Dermal Asthenia (HERDA)

Pages in Study: 84

Candidate for Degree of Doctor of Philosophy

Hereditary Equine Regional Derma Asthenia (HERDA) is a painful disfiguring autosomal recessive skin disorder of Quarter Horse lineages. Affected horses cannot be ridden and most are humanely destroyed. Five years following homozygosity mapping of a putative causal mutation responsible for HERDA, it remains unclear how this mutation causes the HERDA syndrome. HERDA horses have a missense mutation in peptidyl-prolyl cis-trans isomerase B (PPIB) which encodes cyclophilin B (CYPB) and alters folding and post-translational modifications of fibrillar collagen. Loss of function mutations in CYPB recognized in other species classically present as the debilitating bone disease, severe to lethal osteogenesis imperfect (OI). Objectives of this study were to develop a novel method for cryogenic clamping of tendons and ligaments of high tensile strength and validate its performance by ultimate tensile strength testing of normal equine deep digital flexor tendon. This validated method was then used to compare tendon and ligament of HERDA vs. control horses along with great vessels and skin. We hypothesized that all tissues of high fibrillar collagen content would have altered tensile properties due to the CYPB mutation affecting fibrous connective tissue globally within

HERDA horses. Based on previous studies in our laboratory identifying reduced hydroxylysine content and altered collagen crosslink ratios in the skin of HERDA affected animals that implicate lysyl hydroxylase-1 (LH1) dysfunction, we hypothesized that the HERDA PPIB mutation modified an interaction between CYPB and LH1, interfering with hydroxylysine synthesis and its availability for collagen crosslink formation. In addition, we hypothesized that mutant CYPB may also lead to modifications of other known CYPB protein complexes, such as the CYPB, prolyl-3 hydroxylase-1 (P3H1) and cartilage associated protein (CRTAP) triplex. Goals of this study were to investigate the tensile properties of tissues with high fibrillar collagen content from HERDA homozygotes, to elucidate the mechanistic relationship of the HERDA CYPB mutation to the clinical disease, and to provide evidence to substantiate a heterozygote phenotype in HERDA which could be useful to explaining the correlation between lineages that carry the HERDA allele and performance outcomes in the discipline of western cutting competition.

DEDICATION

I would like to dedicate this research to my father, Jack Allen Bowser, for always encouraging me to strive for excellence. Balance grasshopper.

ACKNOWLEDGEMENTS

I would like to first acknowledge the everlasting support and guidance of Dr Cyprianna Swiderski, my mentor these past 6 years. I could not have done this without you, thanks is not enough.

In addition, the other valued members of my committee: Dr Michael Brashier, Dr Steven Elder and Dr Marzia Pasquali. Thank you so much for all your assistance and insights. Research conducted by previous graduate students such as Sally Tipton, Jesse Grady and Ashley Hill has provided the foundation upon which I have added to. And the help of laboratory assistants Nisma Mujahid and Santosh Kumar TK, along with the statistical expertise of Dr Robert Wills is acknowledged with great appreciation.

"If I have seen further it is by standing on the shoulders of giants."

-Sir Isaac Newton

Last, but certainly not least, I must thank my fiancé Basil Hassan Aboul-Enein for always being there for me. I love you with all my heart.

TABLE OF CONTENTS

LIST OF TABLES

LIST OF FIGURES

CHAPTER I

INTRODUCTION

Disease Overview

Hereditary equine regional dermal asthenia (HERDA), originally termed hyperelastosis cutis (HC), was first clinically described by Learner and McCrackin in 1978 (Lerner, 1978). It has since been described in Quarter Horses and related breeds on three continents (Lerner, 1978; Borges, 2005; Rendle, 2008). The disease is characterized by fragile skin that is velvety in texture, loose and hyper-extensible which tears easily and exhibits impaired healing (Lerner, 1978; Hardy, 1988; Pascoe, 1999; Stannard, 2000; White, 2004, 2007). Skin is easily stretched and manipulated, especially along the dorsum of the horse, and predisposes the animal to formation of hematomas, seromas and often severe lacerations from only minor trauma. Clinical signs are often inapparent at birth (Lerner, 1978; Hardy, 1988; Brounts, 2001; White, 2004, 2007) but develop within the first two years of life, often noticed at the time of first saddling (Lerner, 1978; Hardy, 1988; Stannard, 2000). While there is some variation in disease severity (White, 2004; Grady, 2009; Ishikawa, 2012), skin lesions tend to progressively worsen in incidence and severity with age (White, 2004), making HERDA horses unsuitable for riding as well as breeding (Lerner, 1978; Hardy, 1988; Brounts, 2001; White, 2004, 2007). Accordingly, most HERDA horses are humanely euthanized.

Originally suspected to be of autosomal recessive inheritance, extensive pedigree analysis (Hardy, 1988; White, 2004; Rashmir-Raven, 2004) of HERDA affected individuals confirmed (Tryon, 2005) this, along with discovery of consanguinity to a prominent Quarter Horse stallion, Poco Bueno and/or his dam or sire (King and Miss Taylor) (Rashmir-Raven, 2004).

After initial recognition of HERDA as a disease entity in horses, attempts were made to describe histological changes associated with affected animals for diagnostic purposes (Lerner, 1978; Gunson, 1984; Solomons, 1984; Hardy, 1988; Brounts, 2001; Borges, 2005; White, 2004, 2007). Although controversial and subject to pathologic interpretation (Brounts, 2001; Rashmir-Raven, 2004; Borges, 2005), recognition of 'Zonal Dermal Separation' became the initial HERDA diagnostic modality. The discovery of an increased ratio of collagen crosslink degradation products within the urine of HERDA affected horses by Swiderski et al. (Swiderski, 2007) then made non-invasive diagnosis possible at birth, prior to onset of clinical signs of disease. In 2007, homozygosity mapping identified a c.115G>A missense mutation in the gene encoding Cyclophilin B (PPIB) in 64 HERDA affected horses, segregating with inbreeding loops in the genealogy of affected horses (Tryon 2007). This was proposed to be the putative causal mutation for HERDA and heterozygosity for this mutation has now become the standard for identification of both clinically affected and inapparent HERDA carriers (Lee, 2008; Tryon, 2009; Ishikawa, 2012).

The mechanism by which the PPIB mutation leads to the classic skin phenotype seen in HERDA affected horses is still unclear. Cyclophilin B (CYPB) is a member of the peptidyl-proplyl isomerase family of proteins which execute several chaperoning

functions (Steinmann, 1991; Lodish, 1991; Endrich, 1999; Kozlov, 2010) within the endoplasmic reticulum (ER) and Golgi (Zhang, 2003) of cells, including facilitation of the proper folding of collagen proteins (Bachinger, 1987; Liu, 1990; Smith, 1995; Horibe, 2002; Canty, 2005; Ishikawa, 2009). Mutations in CYPB that destroy CYPB function are recognized in other species and classically present as the debilitating bone disease severe to lethal Osteogenesis Imperfecta (Marini, 2007; Choi, 2009; Barnes, 2010; van Dik, 2009; Pyott, 2011), a disorder characterized by osteoporosis, bone fragility, bone deformity, tooth malformations, short stature, and shortened life span (King, 1971). By contrast, to date a clinically evident bone phenotype has not been identified in horses homozygous for the HERDA allele.

The distinctive HERDA phenotype most closely resembles a subtype of a group of the heterogenous inherited connective tissue disorders termed Ehlers-Danlos syndrome (EDS) (Lerner, 1978; Hardy, 1988; Brounts, 2001; White, 2004). This subtype, EDS VIA, is characterized by skin hyperextensibility, articular hypermobility, and tissue fragility (Beighton, 1998; Mao, 2001; Fernandes, 2008). EDS VIA is an autosomal recessive disease caused by mutations in the gene procollagen-lysine, 2-oxoglutarate 5-dioxygenase-1 (PLOD1) which lead to reduced to absent biological activity of the enzyme lysyl hydroxylase-1 (LH1), which PLOD1 encodes (Pousi, 1998; Yeowell, 2000; Walker, 2004). LH1 is responsible for hydroxylation of lysine residues in procollagen peptides (Myllylä, 1988). EDS VIA individuals have significantly decreased procollagen hydroxylysine residues, essential for formation of covalent pyridinium crosslinks, in their collagen (Pasquali, 1997; Mao, 2001; Fernandes, 2008). Furthermore, the ratio between the 2 most common pyridinium crosslinks, deoxypyridinoline (DPD): pyridinoline (PYD)

is greatly increased, which is currently the standard diagnostic screening test for this condition in man (Pasquali, 1994, 1997; Mao, 2001; Fernandes, 2008). Interestingly, we have documented that HERDA affected horses also exhibit reduced total hydroxylysine residues in skin and an increased ratio of DPD: PYD in both skin and urine, (Swiderski, 2006; Hill, 2010) while LH1 activity is normal (Pasquali, unpublished).

Recently, it was found that the HERDA mutated CYPB retains cis-trans isomerization activity, but shows delayed collagen folding and secretion (Ishikawa, 2012) without the increase in lysine hydroxylation, termed over modification, that is typically associated with delay in secretion (Willing, 1988; Cabral, 2007; Christiansen, 2010). The region on the CYPB protein altered by the HERDA mutation appears to be unassociated with cis-trans isomerization catalysis, but with identification of improperly folded proteins in the endoplasmic reticulum (Kozlov, 2010) and LH1 association (Ishikawa, 2012).

While Tryon et al. (2005), through Bayesian statistical methods and meticulous breeding records, estimated the allelic frequency of HERDA to be 1.84% in the Quarter Horse population, the advent of a commercially available genetic test for the HERDA allele has altered this estimate. Subsequently, more recent estimates of the carrier frequency of the disorder within the general United States Quarter Horse breed have been reported at 3.5, 4.2 and 9.2% (Tryon, 2007, 2009; Ishikawa, 2012). Remarkably, in a subset of the Quarter Horse breed, purpose-bred for competition in the western sport of Cutting, this carrier frequency is reported to be 28.3% (Tryon, 2009), as much as nine times higher than the general population. Furthermore, a correlation exists between

cutting lineages that carry the HERDA allele and performance outcomes in this discipline (Tipton, 2008; Equistat.com).

Study Objectives

Goals of this study were to investigate global changes in the tensile properties of HERDA tissues, to elucidate the mechanistic relationship of the mutation to the disease, and to provide evidence to substantiate a heterozygote phenotype in HERDA, explaining the correlation between lineages that carry the HERDA allele and performance outcomes in the discipline of western cutting competition (Tipton, 2008; equistat.com).

The first objective of this study was to determine if the decreased tensile properties previously demonstrated in skin of HERDA horses (Grady, 2009) can be identified in other body tissues of similarly high Type I structural collagen content.

We hypothesized that all tissues of high fibrillar collagen content would have altered tensile properties due to the CYPB mutation affecting fibroblasts globally within HERDA horses. Testing of this hypothesis was through measurement and comparison of tensile strength, elastic modulus, and energy to failure of skin, and great vessels; in addition to comparison of tensile strength of deep and superficial digital flexor tendons and suspensory ligaments of HERDA affected horses compared to unaffected age-matched controls. Facilitation of this study was through first the development of a novel method for cryogenic clamping of tendons and ligaments of high tensile strength and validation of clamp performance by ultimate tensile strength testing of normal equine deep digital flexor tendons.

Building upon prior investigations in our laboratory that identified reduced hydroxylysine content and altered collagen crosslink ratios in the skin and urine of

HERDA affected animals (Swiderski, 2006; Hill, 2010) that are comparable to Lysyl Hydroxylase-1 (LH1) dysfunction, we further hypothesized that the HERDA PPIB mutation modifies an interaction between CYPB and LH1, interfering with hydroxylysine synthesis and its availability for collagen crosslink formation. We also hypothesize that mutant CYPB would show modified binding affinity within other known CYPB protein complexes, such as the CYPB, prolyl-3 hydroxylase-1 (P3H1) and cartilage associated protein (CRTAP) triplex.

CHAPTER II

A CRYOGENIC CLAMPING TECHNIQUE THAT FACILITATES ULTIMATE TENSILE STRENGTH DETERMINATIONS IN TENDONS AND LIGAMENTS

Summary

Objective

To describe the use of a cryogenic clamp of novel design for tensile strength testing of tendinous and ligamentous tissues with inherently high tensile strength. As published in Veterinary Comparative Orthopaedics and Traumatology. 2011;24(5):370-3.

Methods

Inexpensive, easily machined steel clamps were manufactured to facilitate rapid insertion into a standard wedge-screw grip apparatus installed on a Bionix 858 Test System[a] with 2350 L Series Controller[b]. The deep digital flexor tendon (DDFT) of 6 horses was trimmed to a uniform dumbbell shape and secured in clamps using partial submersion in liquid nitrogen for approximately 45 seconds and immediately tested. Approximate time between removal from liquid nitrogen and failure of tendon was 4 minutes.

Results of Study

Failure was achieved in all tendons tested in a region approximating a midpoint between the clamps. Ultimate failure loads of up to 6745 N were achieved without slippage of the tissue from the grips. The ultimate tensile strength of the normal equine DDFT determined in this study was 111.82 +/-11.53 N/mm^2, and the stress versus grip-to-grip elongation plots for our equine DDFT were representative of a standard non-linear elastic curve obtained in similar studies.

Conclusion and Significance

We present a low cost device for quantifying physical properties of specimens with high connective tissue concentrations and inherent high tensile strength. Results of this study indicate that this device provides a practical alternative to other more costly methods of adequately securing larger tendons and ligaments for tensile strength testing.

Introduction

Tensile testing of connective tissues is logistically difficult because low friction at the grip-tissue interface often leads to slippage from the grip before the tendon or ligament ruptures (Rincón, 2001; Riemersma, 1982). Thus, when evaluating tendons and ligaments, the technique by which the tissue is fixed to a uniaxial tension-compression machine is of utmost importance. Clamping techniques that have been employed for high tensile strength tissues include pure mechanical clamps, cryogenic techniques, and combination of mechanical and cryogenic techniques. These techniques, along with their advantages and disadvantages, have been previously summarized (Rincón, 2001; Riemersma, 1982). Systems that utilize the bony attachments of the tendon or ligament as a means of securing one end of the tissue have a primary limitation because they often prevent evaluation of multiple specimens from the same limb. Most testing of high tensile strength connective tissues utilize cryogenic clamping techniques (Riemersma, 1982; Crevier, 1996; Jansen, 1994; Trudel, 2009). The expense of commercial cryogenic clamps precludes their use by many investigators, and some previously described custom cryogenic grips required liquid CO_2 (Riemersma, 1982; Crevier, 1996; Jansen, 1994; Jopp, 2009). In addition, the system we present operates according to the same basic principal as the cyrofixation assembly employed by Trudel et al. to test rabbit Achilles

tendons (Trudel, 2009). However, their system was relatively sophisticated and incorporated double-wall containers into which liquid nitrogen was fed to secure the tendons in a block of frozen saline. In addition, a heater was required to prevent freezing of the tested portion. Therefore, a cryogenic clamp that is inexpensive, simply manufactured, employs a straightforward technique for adequately chilling and fixing tissues to the clamp would be beneficial. We present a novel method for cryogenic clamping of tendons and ligaments of high tensile strength, and validate its performance by presenting data generated during ultimate tensile strength testing of normal equine deep digital flexor tendon. In our laboratory this simple cryogenic clamping method has been used to evaluate differences in the tensile properties of equine tendon and ligament associated with genetic collagen disorders.

Materials and Methods

A photograph of the device used for quantifying strength is shown in Figure 1. Integral to the success of the device are wedge-shaped pads (Figure 2) machined from stainless steel measuring 50.80 mm × 44.45 mm (2.00 in. × 1.75 in.) which clamp together using four 6.4 mm diameter (0.25 inch diameter and 20 threads per inch) socket head machine screws. The opposing surfaces of the clamps were machined in a repeating sinusoidal pattern with a periodicity 12.70 mm (0.50 in.) and peak-to-peak amplitude of 4.44 mm (0.18 in.) to prevent the frozen tissue from slipping. The clamps were manufactured to facilitate rapid insertion into a standard wedge-screw grip apparatus installed on a Bionix 858 Test System[a] with 2350 L Series Controller[b]. The cost to have the grips fabricated by CNC machining was approximately 1,500 USD.

To confirm utility and accuracy of the system, we used the cryogenic grips to determine the ultimate tensile strength of the equine deep digital flexor tendon (DDFT). DDFT were harvested from the forelimbs of 6 Quarter Horses ranging in age from 2-7 years (mean of 4.8 years) which were euthanized for non-orthopedic related conditions. These horses consisted of 4 mares and 2 geldings weighing between 350 and 500 kg. Animals were managed in accordance with a protocol approved by the University Institutional Animal Care and Use Committee. Tendons harvested within 4 hours of death were maintained at -80^{o} C until subjected to mechanical testing. Prior to testing, tendons were thawed at room temperature in a phosphate buffered saline bath. Using a custom template and scalpel each tendon was cut into dumbbell shape, as has been described in other systems (Soslowsky, 2002) so that the ends to be gripped retained their original width of approximately 18 mm, but the width of the section to be tested was reduced to a uniform 6 mm. The gauge section spanned that portion of the tendon which had roughly uniform thickness, and had a minimum length of approximately 30 mm and maximum of approximately 65 mm. Specimen thickness was determined with a Mach-1™ V500cs Micromechanical Test System[c] in analogous fashion to a pressure area micrometer. A plunger lowered onto the tissue at 0.1 mm/sec squeezed the tissue into a rectangular channel, the dimensions of which were recorded when the applied pressure reached 0.1 MPa. Tissue depth was measured at both ends and at the center of the trimmed, 6-mm wide section. Specimen depth was taken as the average of the three measurements. The cross sectional area was calculated as channel width by depth.

Prior to gripping of the tendon, the stainless steel clamps alone were pre-cooled in liquid nitrogen (-195.8°C) for approximately 45 seconds. The full-width ends of the

tendon specimen were then sandwiched between mating jaws of each clamp. Four machine screws at the corners were used to squeeze the specimen between the jaws. Screws were tightened just enough to make the specimen conform completely to the sinusoidal space between opposing grip surfaces so that there were no visible gaps between tendon and grips (Figure 3). This method preserved as much of the specimen's original conformation as possible. The central portion of the specimen, spanning the two clamps, was loosely wrapped in a latex examination glove to prevent splashing onto the exposed tissue and the clamps were partially submerged into liquid nitrogen to a depth approximating 2 cm (Figure 4). Previous investigators have used petroleum jelly to protect the tested portion of the tendon from dehydration and thermal injury, and it could be used in our system as well. The duration of liquid nitrogen submersion resulting in adequate fixation of tissue to the clamps and which did not cause freezing of the tissue that spanned and suspended the clamps was influenced by specimen cross-sectional area. Specimen depth ranging from 6.4 to 8.4 mm required 45-70 seconds of submersion. This timing corresponded to visual observation of partial specimen freezing 1-2mm adjacent to the clamp, at which time the clamps were removed from liquid nitrogen, mounted in the materials testing machine, and the specimen was tested immediately.

Tendons were made taught by applying a preload of 10 N and the distance between clamps (excluding the 1-2mm frozen areas bordering the clamp) defined a specimen's gauge length. In our experiments, this length ranged from 29.17 – 62.69mm (Mean: 45.81). Tendons were distracted at a constant rate of 0.25 mm per second to failure. Force (N) and displacement (mm) data were recorded at 100 Hz. Data was plotted as force versus displacement for each tendon. Time from clamp removal from

liquid nitrogen to tendon failure approximated 4 minutes in all samples. Stress was determined by normalizing the force to cross sectional area. Ultimate tensile strength was defined as the maximum tensile stress.

Results and Discussion

Failure was achieved in all tendons tested at the midpoint between the clamps (Figure 2) and these results are summarized in Table 1. Ultimate failure loads of up to 6745 N were achieved without complete slippage of the tissue from the grips. Some stretch of the tissue within the grips immediately adjacent to the gauge section did occur, but it did not interfere with the ability to achieve failure within the gauge section. This was attributed to the temperature differential at the edge of the grips which allowed the tissue to defrost at this site. As tissue within the grips is expected to be rigid, this could not be accommodated in the mathematical modeling, precluding the calculation of tissue strain from grip-to-grip displacement data. The ultimate tensile strength of the normal equine DDFT determined in this study was 111.82 +/-11.53 N/mm^2 (N/mm^2= MPa), and the 95% confidence interval was [111.82 N/mm^2, 9.23 N/mm^2]. In fact, the entire confidence interval lies between the previously published mean DDFT tensile strengths of 77 MPa (Crevier, 1996) and 133 MPa (Jansen, 1994). Force versus displacement plots for our equine DDFT (Figure 5) are representative of a standard non-linear elastic material curve obtained in similar studies (Crevier, 1996; Jansen, 1994). The method presented herein does not address measurement of local tissue strain which would be required to calculate a specimen's elastic modulus.

Three potential complications of this technique include grip failure due to inadequate freezing of the specimen within the clamps, over-freezing, and limited

working time. Though none of the tendons tested in the experimental group experienced grip failure, we experienced specimen slipping in one instance during development of this technique. In that case, the clamp was re-applied, re-submerged in liquid nitrogen for an additional 15 seconds, and the tendon was successfully pulled to failure. This problem is avoided by precooling the clamps in the liquid nitrogen prior to inserting the specimen, and determining the optimal time for liquid nitrogen immersion to completely freeze the specimen within the clamps. Over-freezing of the sample did not occur and is prevented by optimizing the duration of freezing and close observation. One disadvantage of our gripping method relative to commercial continuously cooled clamps is shorter working time due to eventual thawing of the tissue. However, our experiments were consistently completed within 4 minutes and during this time period thawing of tissue in the clamp was not problematic. Another potential drawback is the trimming of specimens to a dumb-bell shape, which would preclude testing tissues with focal lesions. However, slightly smaller tendons and ligaments could be tested intact. Larger tendons such as the equine DDFT could possibly be tested intact using larger grips with a longer sine-wave period. Based on the results of this study, the cryogenic clamping technique presented herein will be useful for comparing the tensile strength of tendons from horses and other animals where global differences in the tissue composition would be expected such as with collagen disorders.

A primary advantage of this gripping system is the use of a sinuous gap between the grip surfaces which, when combined with freezing, makes this device highly resistant to slippage. Attempts to test the tissue using conventional flat-faced grips with a grooved surface always resulted in slippage under tissue compression that was as high as could be

achieved manually. Therefore we speculate that freezing the tissue in the wavy pattern achieved fixation with less tissue compression than would have been required using conventional, non-freezing grips. This is significant because excess compression pressure that characterizes many clamping methods leads to increased deformation of the clamped portions of the specimen. This creates unequal fiber lengths within the specimen itself, causing uneven load distribution (Riemersma, 1982). We believe the freezing method described herein may serve to mitigate this effect because the fixation does not rely on extremely tight squeezing between the grips. Also significant is the wedge-screw apparatus, which facilitates rapid mounting of the specimen in the servohydraulic testing machine. This effectively minimizes the time from freezing to initiating a test. Although preconditioning was not performed in the current study, the tissue remained frozen for several minutes after mounting which would have been ample time for more sophisticated loading protocols. Finally, the design of previously described cryogenic clamps is significantly more complicated, requiring constant circulation of liquid CO_2 (Riemersma, 1982; Crevier, 1996; Jansen, 1994) through the clamping device to maintain freezing. Our clamp method avoids the need for constant cooling, simplifying the manufacture of this device. Liquid nitrogen is relatively inexpensive and is readily available at most research-intensive institutions. In our assays, after accounting for recovery and reuse of residual liquid nitrogen following each assay, 10L was sufficient to perform at least 25 tests.

In conclusion, this device provides an inexpensive and effective method for quantifying physical properties of specimens with high connective tissue concentrations and inherent high tensile strength that lead to specimen slippage during uniaxial

tension/compression testing. This device incorporates inexpensive, easily machined steel clamps in which the tissue is held securely by freezing it into a serpentine shape using liquid nitrogen. Our results substantiate that this device provides a practical alternative to other more costly methods of securing larger tendons and ligaments for tensile strength testing.

Table 1 Load and Tensile Strength Determinations for Deep Digital Flexor Tendon Obtained from Six Normal Horses Using the Described Clamp Apparatus.

Horse	Thickness (mm)	Cross-Sectional Area (mm^2)	Spec Gauge Length (mm)	Load (N)	Ultimate Tensile Stress (MPa)
1	6.38	38.27	62.29	4524.7	111.71
2	7.96	47.79	35.26	5226.4	103.34
3	6.61	39.68	29.17	4677.6	111.38
4	7.58	45.47	44.27	5903.2	122.66
5	8.41	50.45	52.92	6744.7	126.31
6	7.75	46.53	50.92	4704.6	95.54
Average	7.45	44.7	45.81	5296.9	111.82
Standard Deviation	0.79	4.76	12.16	871.7	11.53

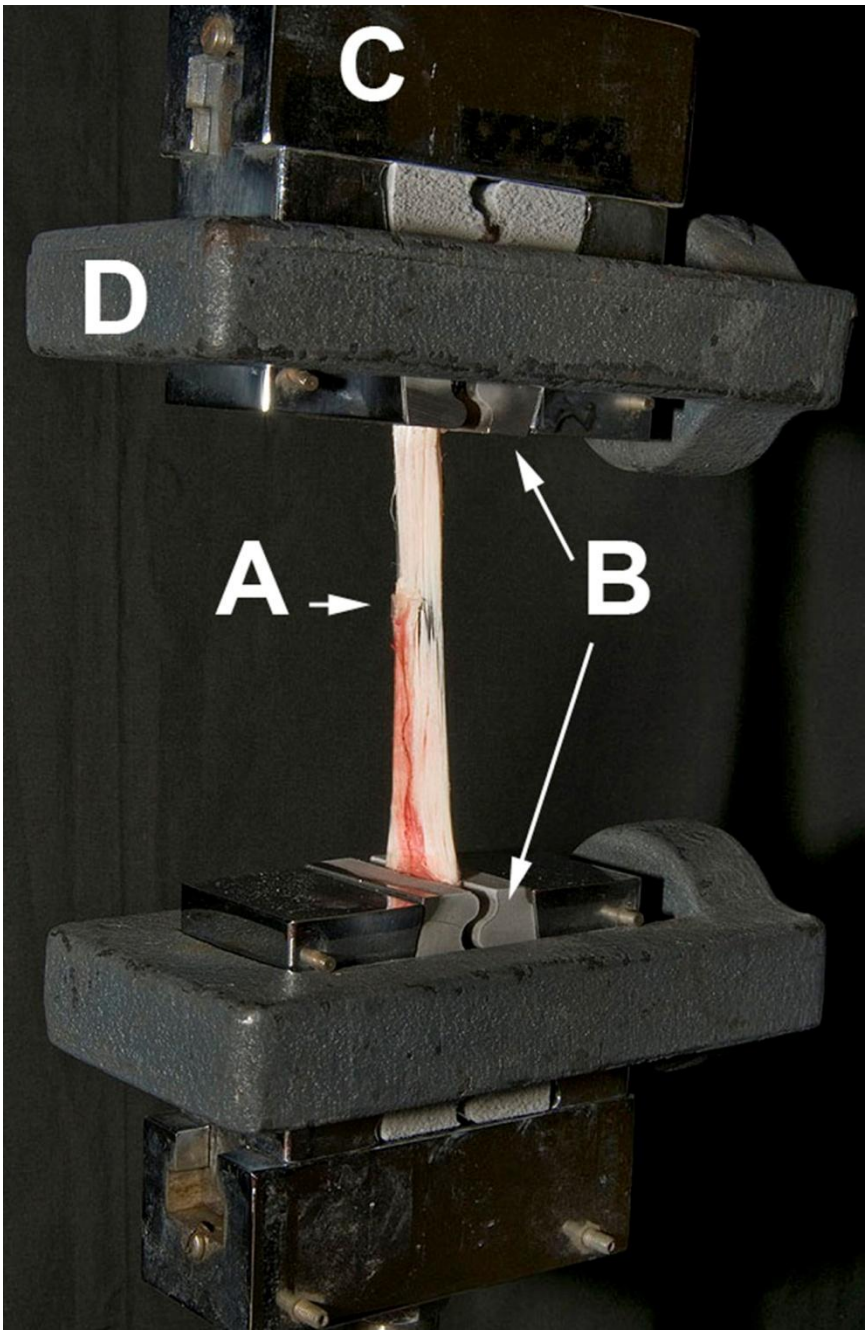

Figure 1 Photograph of the Manufactured Clamps Mounted on the Bionix Test System.

The mounted specimen, an equine deep digital flexor tendon (**A**), demonstrates failure (small arrow) that is equidistant from the clamps (**B**). Clamps are securely mounted in the wedge-shaped receiver of the test machine (**C** and **D**).

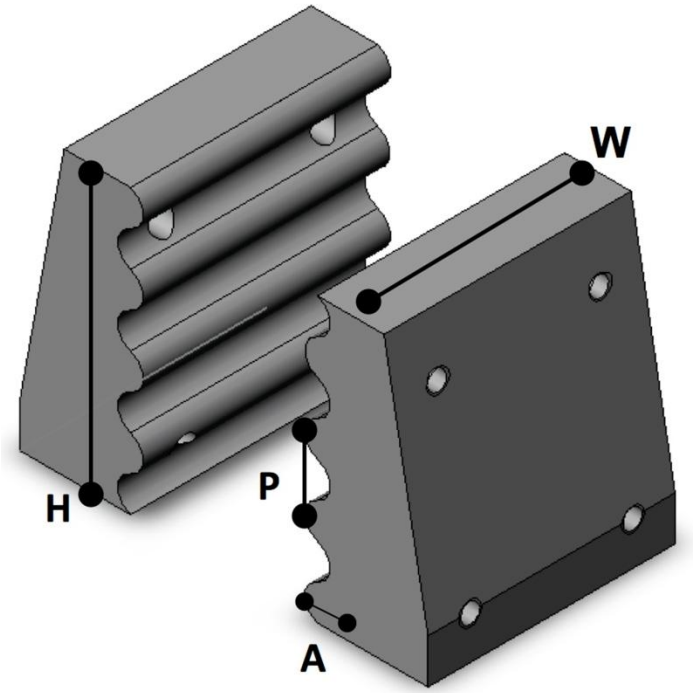

Figure 2 Schematic Drawing of Wedge-Shaped Clamp Pads Machined from Stainless Steel.

Height (**H**) is 50.80 mm × 44.45 mm width (**W**) (2.00 in. × 1.75 in.). The specimen is secured within the pads using four 6.4 mm diameter (0.25 inch diameter, 20 threads per inch) socket head machine screws. The opposing surfaces of the clamps were machined in a repeating sinusoidal pattern with a periodicity (**P**) of 12.70 mm (0.50 in.) and peak-to-peak amplitude (**A**) of 4.44 mm (0.18 in.).

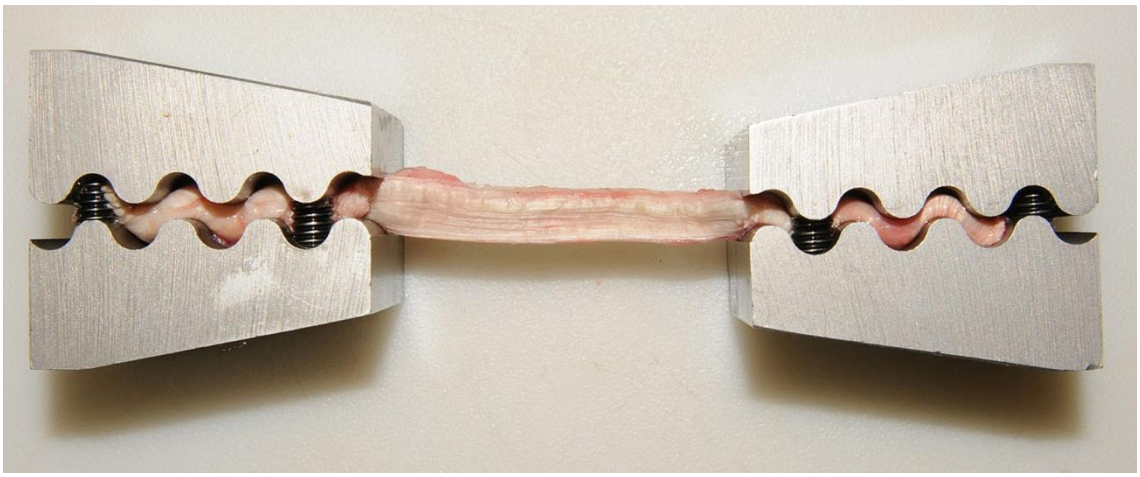

Figure 3 Specimen Mounted in the Wedge-Shaped Clamp Pads.

Sufficient compression is achieved to slightly conform the tendon to the sinusoidal contour of the clamping surface.

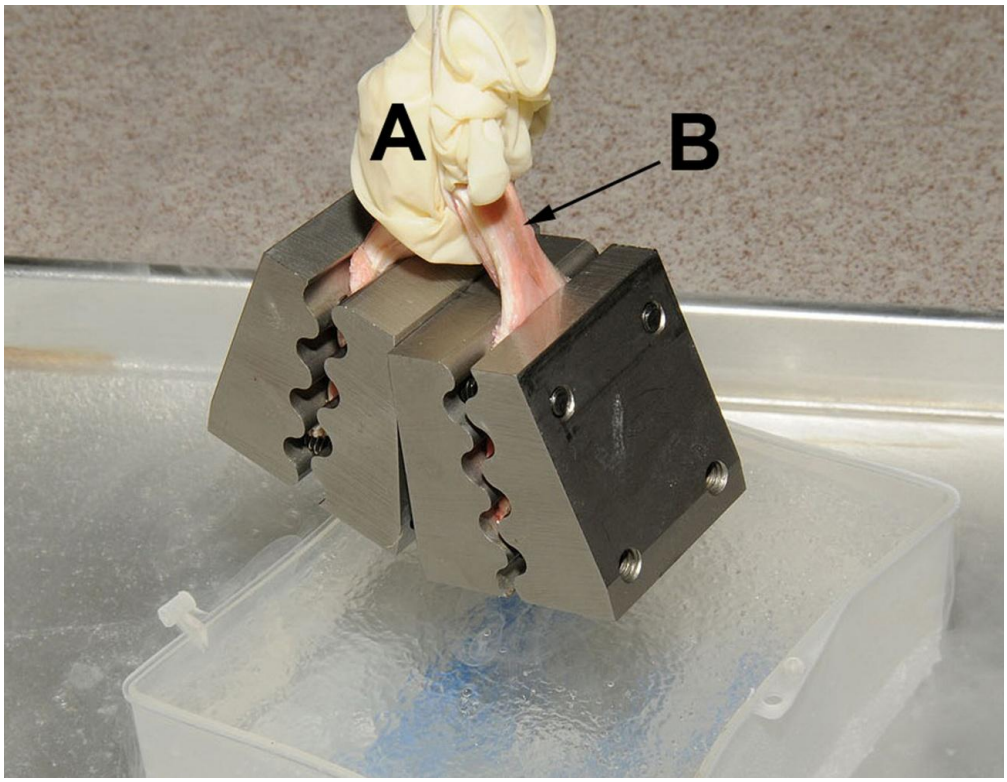

Figure 4 Clamp Submersion into Liquid Nitrogen.

Clamps are submersed to a depth approximating 2cm by suspending the specimen from a wire. An exam glove (**A**) loosely wrapped around exposed tendon (**B**) to prevent excessive splashing.

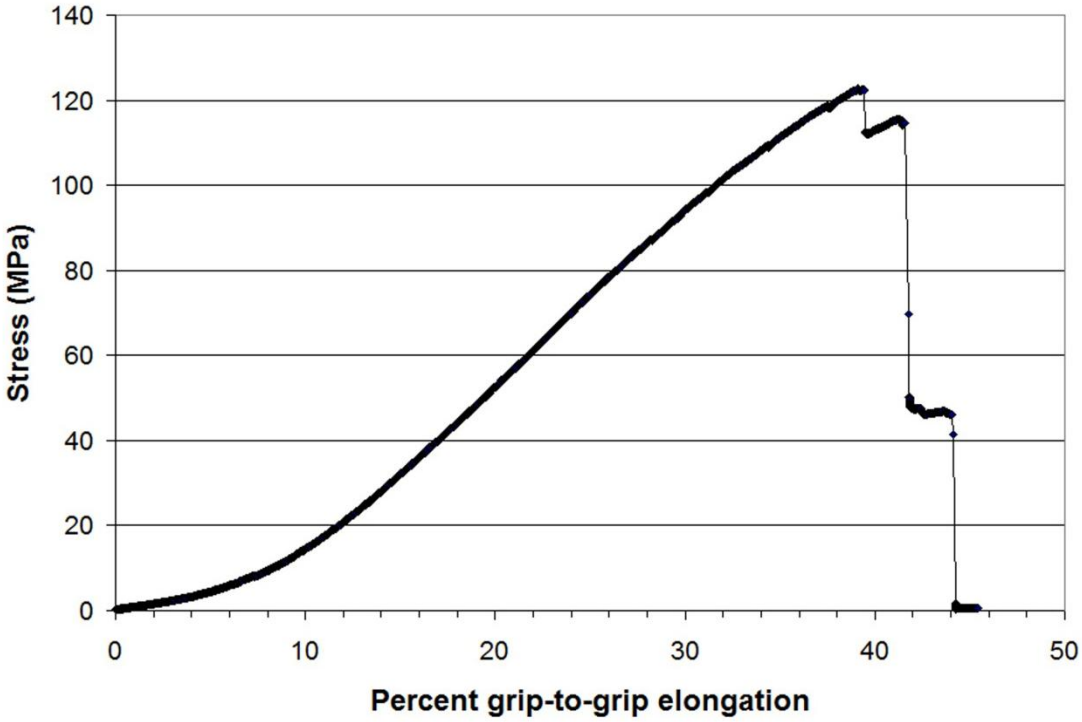

Figure 5 Representative Stress vs. Elongation curve obtained from Tensile Strength Testing of Equine Deep Digital Flexor Tendons using Described Method.

CHAPTER III

TENSILE PROPERTIES IN COLLAGEN RICH TISSUES OF QUARTER HORSES WITH HEREDITARY EQUINE REGIONAL DERMAL ASTHENIA

Summary

Objective

Hereditary Equine Regional Dermal Asthenia (HERDA) is an autosomal recessive disorder of Quarter Horses characterized by skin fragility. HERDA horses have a missense mutation in peptidyl-prolyl cis-trans isomerase B (PPIB) which encodes Cyclophilin B (CYPB) and alters folding and post-translational modifications of fibrillar collagen. We hypothesize that tendon, ligament, and great vessels, which like skin are rich in fibrillar collagen, will also have abnormal biomechanical properties in HERDA horses.

Methods

Forelimb suspensory ligament, superficial and deep digital flexor tendons; withers, forelimb, and abdominal skin; main pulmonary artery and the aortic arch were harvested from six HERDA and six age-matched control horses without the HERDA allele. Tissues were distracted to failure. Tensile strength (TS) for all tissues, and elastic modulus (EM) and energy to failure (ETF) for skin and vessels were compared.

Study Results

HERDA horses had significantly lower TS and EM in tendinoligamentous tissues and great vessels, respectively. TS, EM and ETF were significantly lower in HERDA skin. Differences in TS and ETF were more extreme at the withers than the forelimb or abdomen.

Conclusion and Significance

Tendinoligamentous tissue, great vessels, and skin are significantly weaker in horses with HERDA than horses lacking the PPIB mutation, substantiating that diverse tissues with high fibrillar collagen content are abnormal in HERDA and the HERDA phenotype is not limited to the integument.

Introduction

Hereditary equine regional dermal asthenia (HERDA) is an autosomal recessive disorder which is characterized by fragile skin that is loose, hyper-extensible and easily torn (Lerner, 1978; Stannard, 2000; White, 2004, 2007; Tryon, 2005). Horses with HERDA develop seromas, hematomas, and ulcerations primarily along their dorsum (Stannard, 2000; White, 2004, 2007). Clinical signs have been reported as early as 2 months of age, but most HERDA affected horses are diagnosed around the time of their first saddling, at approximately 18 months of age (White, 2004, 2007). While there is some variation in disease severity, skin lesions tend to progressively worsen in incidence and severity with age, making HERDA horses unsuitable for riding as well as breeding. Accordingly, most HERDA horses are humanely euthanized.

HERDA affects Quarter Horse lineages tracing to the sire Poco Bueno and/or his dam Miss Taylor (Rashmir-Raven, 2004). Line breeding of these lineages, which are popular in certain performance disciplines, is credited with concentrating the recessive HERDA allele within the respective disciplines (Tipton, 2008; Tryon, 2009). Homozygosity mapping identified a c.115G>A missense mutation in the gene encoding Cyclophilin B (PPIB) in 64 HERDA affected horses, segregating with inbreeding loops in the genealogy of affected horses (Tryon, 2007). Heterozygosity for this mutation is used to identify inapparent HERDA carriers (Lee, 2008; Tryon, 2009). Tryon et al. (2009) estimated the allelic frequency of HERDA to be 0.142, corresponding to a 28% carrier rate in the cutting horse subpopulation versus an allelic frequency of .021 (4% carrier rate) in the Quarter Horse population.

CYPB is a member of the peptidyl-prolyl cis-trans isomerase family of proteins which catalyze prolyl-containing bonds in procollagen to the trans configuration. This trans configuration is required to form the triple helical collagen molecule (Bachinger, 1987). Conventionally viewed as the primary rate limiting enzyme in fibrillar collagen synthesis, CYPB also has critical functions in procollagen trafficking, processing, and chain association (Canty, 2005; Pyott, 2011). The HERDA mutation does not alter prolyl isomerization activity of CYPB but delays collagen folding and secretion and modifies a region of CYPB that identifies improperly folded proteins in the endoplasmic reticulum, events presumed to alter collagen organization (Tryon, 2007; Ishikawa, 2012; Kozlov, 2010). Despite the global nature of this pathophysiologic mechanism, clinical manifestation of HERDA is restricted to the integument (White, 2007; Mochal, 2010). Prior description of significantly reduced tensile strength (TS), elastic modulus (EM) and

energy to failure (ETF) in HERDA skin (Grady, 2009) where Types I and III fibrillar collagen predominate in a 4:1 ratio (Lovell, 1987), lead us to hypothesize that the HERDA phenotype extends beyond the integument to alter biomechanical properties of diverse tissues with high fibrillar collagen content including tendon, ligament and great vessels. Our findings indicate that the HERDA Cyclophilin B mutation results in global alterations in fibrillar collagen molecule assembly, folding and fibril organization that modify the mechanical properties of fibrous tissues, even when clinical signs are not evident. This finding is of broad scientific relevance to deciphering the molecular events that determine tensile properties of fibrous tissues. The potential relevance of these findings to the over-representation of the HERDA allele in cutting horses with elite performance is discussed.

We have previously demonstrated that tensile strength (TS), elastic modulus (EM) and energy to failure (ETF) are significantly reduced in the skin of HERDA affected horses (Grady, 2009). Skin is composed of predominantly Types I and III fibrillar collagens in a 4:1 ratio (Epstein, 1978; Lovell, 1987). This study investigated the hypothesis that the HERDA phenotype extends beyond the integument to alter biomechanical properties of diverse tissues with high fibrillar collagen content including tendon, ligament and great vessels.

Materials and Methods

Animals

Six Quarter Horses with HERDA were identified by compatible skin lesions, co-sanguinity for the implicated lineage, and homozygosity for the c.115G>A missense mutation in PPIB. Six control horses that had normal skin, and lacked the PPIB mutation

included 4 Quarter Horses, one Quarter Horse cross and one Tennessee Walking-Horse euthanized for conditions that did not affect the structural integrity of the tissues of interest. HERDA genotyping was performed at Cornell University Animal Health Diagnostic Laboratory[d]. HERDA horses (4 geldings, 2 mares) were between 1.5 and 7 years old (mean 4.6). Control horses (2 geldings, 4 mares) ranged from 2-7 years of age (mean 4.8). Investigations were approved by the University Institutional Animal Care and Use Committee.

Tissue Collection

Full-thickness skin samples were harvested from withers, forelimb, and abdomen using a dumbbell-shaped template as described (Grady, 2009). Great vessels were transected 2 cm distal to the heart and 30 cm and 20 cm distal to this site in the aorta and pulmonic artery, respectively. Forelimb superficial digital flexor tendon (SFT) and deep digital flexor tendon (DFT) were transected proximally at the musculotendinous junction and distally at the diaphysis of the proximal phalanx. The forelimb suspensory ligament (SL) was transected at its origin on the palmar surface of the third metacarpal bone and distally at each insertion with the proximal sesamoid bone. Tissues were collected within 4 hours of euthanasia, placed into evacuated whirl paks[e], and stored at -80° C until assayed.

Tissue Preparation and Thickness Determination

Tissue thickness was determined prior to tensile testing with a Mach-1™ V500cs Micromechanical Test System[c] as described previously (Grady, 2009; Bowser, 2011). Skin that was harvested in the requisite template shape during collection and frozen was

equilibrated to room temperature. Tendon and ligament (SFT, DFT, SL) were thawed at room temperature in phosphate buffered saline and cut to a dumbbell shape using a custom template such that the tissue ends to be gripped during mechanical testing retained their original dimensions. The body of the tissue spanning the gauge length measured 6 mm wide. Gauge length, which is not a factor in calculations of tensile strength, was standardized at 4 cm for tendons and ligaments based upon results from preliminary experiments (Bowser, 2011). Tendons and ligaments with these dimensions consistently met ASM international criteria for uniaxial tensile testing: failure in the middle third of the gauge length and that the square root of the cross-sectional area: gauge length did not vary between groups (variance, σ^2 <0.03%), which is critical for comparisons of elongation (Davis, 2004). Grip to grip distance for all tendinoligamentous structures varied slightly according to height of the animal and total length of the dissected specimen. Skin was harvested in the previously described dumbbell template (Grady, 2009) during collection to achieve a width of 1 cm and gauge length of 6 cm was equilibrated to room temperature. Vessels were also brought to room temperature and were incised longitudinally to 'unroll' each vessel. Dumbbell shaped samples were cut using a template so that the width and length of the section to be tested were 6.5 mm and 3 cm, respectively.

Following instrument calibration, skin and vessel thickness were determined using a 42mm diameter circular plate lowered at 25 μm•s-1 until the sample provided 50 g of compressive resistance, reflecting an applied stress of approximately 1 KPa. For tendons and ligaments, a cuboidal plunger was lowered at 0.1 mm•s-1, squeezing the tissue into a rectangular cross section. Tissue dimensions were recorded when the applied

pressure reached 0.1 MPa and specimen thickness was determined at both ends and centrally. Thickness was recorded as the average of the three measurements.

Determination of Tensile Properties

TS, EM, and ETF were determined for skin and vessels using an Instron® 1011 Universal Testing Instrument[f] as previously described (Grady, 2009). Wire mesh was secured to the dumbbell ends of each sample using cyanoacrylic and samples were mounted in the grips of the testing machine. Preloads of 1 newton (N) were applied to skin samples and 0.5 N to vessels. Grip-to-grip distance and sample width were determined with a digital micrometer. Skin was assayed using a 1000 N load beam in conjunction with Instron® Series IX software[f] to measure displacement (mm) and force (N) of the skin samples as they were loaded at a constant rate of 10 mm•min-1 with a data recording rate of 10 points per second until failure. The aorta and pulmonary artery were similarly assayed using a load beam of 50 N and sample loading at a constant rate of 20 mm•min-1. TS of tendons and ligaments was determined using a Bionix 858 Test System[a] with 2350 L Series Controller[b] and purpose-made stainless steel cryogenic clamps as previously described (Bowser, 2011). A preload of 10 N was applied to the mounted tissue, and grip to grip distance and sample width were measured immediately prior to distraction at a constant rate of 0.25 mm•s-1 to failure. Force (N) and displacement (mm) data were recorded at 100 Hz. To determine stress for all samples, force (N) was normalized to sample cross-sectional area. TS was the maximum tensile stress (in mega-Pascals [MPa]). For skin and vessels, sample elongation was normalized to starting grip-to-grip length to determine strain. Strain at failure was calculated as the percent elongation of each tissue at the point of maximal tensile stress. Skin and vessel

EM (in MPa) were calculated as the best-fit line through the linear portion of the stress versus strain curve. Skin and vessel ETF in millijoules per millimeter cubed (mJ/mm3) were calculated as the area under the stress vs. strain curve to the point of failure (defined as the point of maximum tensile stress).

Statistical Analysis

Outcome data (TS, EM, and ETF) approximated the normal distribution for all tissues using q-q plots and the UNIVARIATE procedure in SAS[g] software for Windows 9.2. Mixed model analysis within each tissue group for each outcome used the GLIMMIX procedure where disease status, location, the disease status x location interaction, sex, and age were fixed effects and horse identity was a random effect. The threshold for significance was $p \leq 0.05$. If non-significant, sex and/or age were removed from the model. Differences in least square means were used for pairwise comparisons among locations if location was significant and between HERDA and control skin values at each location within a tissue group if disease status by location interaction was significant.

Results of Study

Animals

EM was significantly higher in the skin of geldings compared to mares ($p=0.0318$). Sex and age were not significantly associated with TS or ETF of skin or with any measures in the other tissues. Tensile values and fixed effect p-values of tissues from HERDA vs. control horses are represented in Table 2. Typical stress vs. strain curves for

skin (withers) and vessel (aorta), and a typical stress vs. grip to grip elongation curve for tendioligaments (SFT) of control versus HERDA animals is shown in Figure 6A-C.

Skin Samples

TS ($p=0.202$), EM ($p=0.489$), and ETF ($p=0.111$) were not significantly different across skin locations (withers, abdomen, and forelimb). HERDA skin had significantly lower TS, EM, and ETF than did control skin ($p<0.001$, Figure 7A-C, Table 2). The interaction of location and disease status approached significance for TS ($p=0.053$) and ETF ($p=0.055$) but not for EM ($p=0.968$). Pairwise comparisons of HERDA and control skin at different locations revealed that although HERDA skin consistently had lower TS, the difference was more extreme at the withers ($p<0.001$) than at the forelimb ($p=0.034$) or abdomen (0.068). Similarly, the differences in ETF were consistently lower in HERDA skin but were more extreme at the withers ($p<0.001$) than at the forelimb ($p=0.039$) or abdomen (0.433). Differences in EM were similar at each of the three locations resulting in a non-significant interaction term.

Vessel Samples

TS ($p=0.018$) and EM ($p=0.006$) were significantly lower in the aorta than pulmonary artery while the difference in ETF, also lower in the aorta, was not statistically significant ($p=0.079$) (Table 2). The EM in vessels from HERDA horses was significantly lower ($p=0.039$) than in vessels from control horses. Lower TS and ETF observed in vessels from HERDA horses relative to controls were not statistically significant. The disease status by location interaction term was not significant for TS

(p=0.881), EM (p=0.326), or ETF (p=0.487) indicating the significantly lower EM seen in HERDA horses was consistent in both the aorta and pulmonary artery.

Tendinoligamentous Samples:

Location was significantly associated with TS (p<0.001). Pairwise comparisons demonstrated that although SL had significantly lower TS than DFT (p<0.001) or SFT (p<0.001) (Table 2), TS of DFT and SFT were not significantly different (p=0.2657). TS was significantly lower in tendinoligamentous structures of HERDA horses compared to control horses (p=0.016) (Figure 8). The disease status by location interaction term was not significant for TS (p=0.577), indicating the differences seen between HERDA and control horses were consistent across the tendinoligamentous structures that were examined.

Discussion

More than 25 Types of collagen result from unique combinations of 3 polypeptide chains that fold together, forming the characteristic triple-helical collagen molecule (Miller, 1976; Fratzel, 2008). Fibrillar collagens, Types I, II, III, V, and XI, are the structural building blocks of tissue and share similar microscopic structure in which collagen molecules arrange in a highly ordered staggered pattern to form fibrils (Miller, 1976). Within fibrils, pyridinoline and deoxypyridinoline are intermolecular cross-links that covalently bind the ends of the staggered collagen molecules, imparting tensile strength (Fratzel, 2008). Relative quantities and distinctive physical characteristics of the collagen Types in a tissue constitute a collagen fingerprint that, together with collagen-matrix interactions, shape the biomechanical properties and suitability of tissues for

biological functions (Miller, 1976; Fratzel, 2008; Dombi, 1993). Bone collagen is almost exclusively Type I collagen (Fratzel, 2008) and is composed of two α-1 chains and one α-2 chain. In their triple helix conformation, these chains produce collagen fibrils of large diameter that form thick fiber bundles with high resistance to deformation. By contrast, Type III collagen is comprised of three identical α-1 chains which align compactly, creating a smaller fibril diameter that functions as a fine mesh and imparts pliability to tissue (Fratzel, 2008). Differences between the biomechanical properties of HERDA and normal tissues reflect differences in tissue structural collagen that are relevant to understanding how the PPIB mutation impacts the HERDA phenotype.

We expand on prior observation of decreased strength and increased distensibility of HERDA skin (Grady, 2009) by demonstrating significantly weaker biomechanical properties of great vessels and tendinoligamentous tissues from HERDA horses. Like skin, these tissues have a predominance of Type I collagen with lesser quantities of Type III collagen. Prior investigations of HERDA horses also identified thinning and ulceration in HERDA corneas (Mochal, 2010), a tissue composed of a highly organized matrix of Type I and V collagen (Fratzel, 2008), indicating that HERDA cornea possesses clinically significant alterations in biomechanical properties. Therefore, the HERDA phenotype includes abnormal biomechanical properties in diverse tissues with high fibrillar collagen content, though clinical manifestations have been identified only in integumentary tissues with very high Type I collagen content.

Consistent with Grady et al. (2009), we identify highly significant ($p<0.001$) decreases in TS, ETF and EM in skin of horses with HERDA which are not restricted to dorsal regions of the body. Unique to this report is recognition that the magnitude of

difference in biomechanical properties between HERDA and control skin varies significantly with the region of the skin that is tested. Differences in TS and ETF were more extreme in skin from the dorsum ($p<0.001$), than forelimb ($p=0.034$ and 0.039) or abdomen ($p=0.068$ and 0.443). The greater disparity in strength of HERDA and normal skin along the dorsum may explain why lesions are more common on the dorsal skin of horses with HERDA relative to skin on dependent regions (Lerner, 1978; White, 2004, 2007) which are naturally susceptible to trauma and pressure during ventral recumbence.

In addition to three regions of the skin, tensile properties of great vessels were chosen for their similarities in collagen composition. Elastic modulus was significantly reduced in HERDA vessels and the magnitude of this decrease was equivalent in both aorta and pulmonary artery, indicating that HERDA vessels are more extensible than normal vessels. Though mean TS and ETF were lower in HERDA than control horses for both aorta and pulmonic artery, these differences did not meet the threshold of significance. Biomechanical properties of HERDA and control vessels in this investigation predict the ability to identify significant differences (power: 0.8, $p< 0.05$) between groups in the aorta and pulmonary artery with a sample size >11 horses per group. Disparity between collagen fiber alignment in the vascular parenchyma and the orientation of distractive forces applied in our method was a potential confounding factor because in vivo forces at the vascular wall primarily radiate axially, influencing collagen alignment (Fratzel, 2008; Azadani, 2012). Axial expansion, which simulates vascular filling, may be more appropriate to assess the tensile properties of vessels. In both HERDA and control horses, the UTS and EM of aorta are significantly lower than

pulmonic artery, consistent with increased extensibility that is essential for accommodating changes in systemic blood pressure (Azadani, 2012).

Collagen constitutes 20-30% of human blood vessels (Hosoda, 1984; Barnes, 1985; Bishop, 1990), less than half of the content of skin (70%) (Lovell, 1987; Dombi, 1993), tendon (75%) or ligament (60%) (Amiel, 1984; Birch, 2008). The Type I: Type III collagen ratio is also reduced in blood vessels (approximately 2:1) relative to other tissues (Hosoda, 1984; Barnes, 1985; Lovell, 1987; Bishop, 1990). Type I collagen molecules create large diameter fibrils that form thick fiber bundles with high resistance to deformation. By contrast, Type III collagen molecules align compactly, creating a smaller fibril diameter that functions as a fine mesh and imparts pliability to tissue (Fratzel, 2008). Congruent with Type I collagen's strength, tensile differences between groups in tissues with comparatively lower total and Type I collagen should be more subtle than tissues with comparatively higher Type I collagen content. Relative to HERDA skin, where clinical signs are associated with a 56-80% decrease in TS (Grady, 2009), the observed TS decrease in aorta and pulmonic artery, where clinical abnormalities have not been described, were 42 and 29%, respectively. Collectively, these findings suggest that absence of vascular abnormalities in HERDA horses likely reflect an insufficient magnitude of reduction in vessel strength. This could potentially be overcome at extreme pressures. Vascular injury, including arterial rupture, is reported in horses and certain human collagen disorders (Fratzel, 2008; Fernandes, 2008; Ploeg, 2012), but has not been documented in association with the HERDA allele.

The TS of tendinoligamentous structures was significantly reduced in HERDA horses relative to controls ($p=0.016$), which was consistent across SFT, DFT and SL.

This difference represented an 18%, 9% and 21% decrease from control values for SFT, DFT and SL, respectively. We do not report EM and ETF for these structures because a degree of stretch was identified at the edge of the grips where the temperature differential was greatest, which could not be accounted for because tissue within the grips is fundamentally expected to be rigid. Strain, as determined from grip-to-grip displacement, could not be used to calculate EM and ETF. However, ultimate tensile strength is equal to force per unit cross sectional area, and is independent of tissue elongation if the test material fails uniformly in the middle third of the gauge length (Davis, 2004). All tendinoligamentous structures failed in their midsubstance in this investigation and we have previously substantiated that UTS of normal equine tendon assayed identically agrees with published values from differing experimental approaches (Bowser, 2011; Jansen 1994; Crevier, 1996).

Although EM could not be calculated for tendinoligamentous structures, multiple investigators have documented that as UTS decreases, EM also decreases in these structures (Thorpe, 2012, 2010; Souza, 2010). Thorpe et al (2010) specifically demonstrated a direct positive correlation between UTS, EM and yield stress in equine tendon that is highly significant $p<0.001$. Skin and vessels have a similar collagen composition to tendinoligamentous structures, making trends in their tensile properties of relevance. Total collagen in tendon, ligament, skin and vessel consists of 95%, 90%, 85% and 70% Type I collagen respectively; the remainder is primarily Type III collagen (Amiel, 1984; Birch, 2008; Lovell, 1987; Hosoda, 1984; Smith, 2005). In this study HERDA skin had significantly reduced TS and significantly reduced EM when compared to control skin. HERDA vessels also had significantly reduced EM and although not

statistically significant, TS was also lower in HERDA vessels. Collectively these findings suggest that EM would also be positively correlated to UTS in tendinoligamentous structures in HERDA horses.

To our knowledge increased incidence of tendinoligamentous injury in HERDA homozygotes is not reported. However, skin fragility precludes rigorous training or high level competition with the weight of a rider, important risk factors for tendinoligamentous injury (Minetti, 1999; Smith, 2005). Our review of the medical records of 52 adult HERDA horses maintained on pasture at Mississippi State University College of Veterinary Medicine from 2 months to 8 years duration within the time period between 1996 and 2009 did not identify the occurrence of clinically evident tendinoligamentous injuries. This agrees with reported clinical findings of a HERDA affected foal in the first 1.5 years of life, where training on a lunge line at 14 months of age did not reveal joint laxity or orthopedic abnormalities (White, 2007). In light of recent evidence supporting global abnormalities in fibrillar collagen synthesis in HERDA (Ishikawa, 2012), determining how the HERDA PPIB mutation enables decreased TS of tendinoligamentous structures without overt clinical disease, while accounting for decreased TS and overt disease in integumentary tissue, are clinical features that warrant investigation.

Congruent with the HERDA phenotype that is characterized by trends in reduced TS and EM of tissues with substantial fibrillar collagen content, Thorpe et al (2012) recently demonstrated this same pattern in comparisons of the tensile properties of energy storing tendons relative to positional tendons with similar Type I collagen composition. TS and EM were significantly lower in energy storing tendons, which store potential

energy during stretch in the stance phase of the stride and release energy during recoil in the swing phase of the stride. This high level extension and recoil increases locomotor efficiency by as much as 36% during high speed locomotion in the horse (Thorpe, 2012), decreasing the energetic costs of muscular work (Minetti, 1999).

Our investigation was designed to determine if the HERDA mutation causes global changes in tensile properties of Type I collagen rich tissues that could increase their capacity to store potential energy. This is of interest because the HERDA allele is segregated within the western performance discipline of cutting. The HERDA carrier frequency is 28.3% in cutting horses, versus 3.5% in the Quarter Horse population (Tryon, 2007, 2009). Horses that are heterozygous for the HERDA allele do not have overt evidence of the HERDA phenotype, are over-represented among cutting horses with elite performance, and a correlation exists between cutting lineages that carry the HERDA allele and performance outcomes in this discipline (Tipton, 2008; equistat.com).

Cutting horses prevent a calf from rejoining a group of calves situated to the rear of the horse. The horse mirrors the movements of the calf, necessitating successions of rapid turns with rapid and unpredictable side-to-side accelerations and decelerations. Locomotion of this nature has a high energetic cost. Stretch of energy storing tendons during loading followed by recoil when unloaded can substantially increase locomotor efficiency (Thorpe, 2012), decreasing this energetic cost of locomotion (Minetti, 1999). This ability of a tendon to store potential energy is associated with reduced TS and EM, reflecting the need to be more extensible (Thorpe, 2012). Interestingly, variable heterozygote phenotypes with subtle signs of the homozygous phenotype have been identified in investigations of PARKIN and PINK1, mutations that cause autosomal

recessive Parkinson's disease (Abbas, 1999; Zhang, 2000; Tan, 2003; Valente, 2004; Khan, 2005; Hedrich, 2006; Dagda, 2009). These heterozygotes have a spectrum lacking overt clinical disease, despite cellular evidence of dopaminergic dysfunction and subtle extrapyramidal signs of which the patient is not aware. These collective findings: decreased UTS of tendinoligamentous tissues, decreased EM and UTS in tissues with a similar collagen composition to tendon and ligament, strong positive correlation between reductions in UTS and EM that improve locomotor efficiency of tendon, and subtle manifestations of human homozygous recessive disease phenotypes in heterozygotes carrying the recessive allele, lead us to hypothesize that the performance advantage and positive selection of HERDA heterozygotes in cutting may reflect altered biomechanical properties of collagenous structures including tendons and ligaments that improve the locomotor efficiency of HERDA heterozygotes in this discipline.

CYPB catalyzes isomerization of proline residues to the trans- configuration during procollagen synthesis, which is required for procollagen chain association to form the triple helical collagen molecule. This is considered the rate limiting step in collagen synthesis (Bachinger, 1987; Pyott, 2011). However, HERDA CYPB maintains normal prolyl-isomerization activity, substantiating that the mutation does not modify the cis-trans isomerase catalytic region of CYPB, yet collagen folding and secretion are delayed (Tryon, 2007; Ishikawa, 2012). Instead, the mutation modifies a region of CYPB that identifies improperly folded proteins in the endoplasmic reticulum, events presumed to alter collagen organization (Ishikawa, 2012). Decreased TS of tissues with a predominance of Types I and III collagen identified in this investigation support this proposed mechanism. Our findings indicate that abnormal posttranslational modification

and disorganization of Type I and/or III collagens (and likely other fibrillar collagens) contribute to the HERDA phenotype by modifying the biomechanical properties of tissues rich in these collagens, even in the absence of clinical abnormalities.

Bone collagen is highly enriched for Type I collagen and both humans and mice lacking CYPB have severe to lethal bone fragility (Van Dik, 2009; Choi, 2009; Barnes, 2010; Vranka, 2010; Pyott, 2011). By contrast, a clinically evident bone phenotype has not been identified in association with the HERDA allele. This indicates that the HERDA CYPB mutation modifies the biochemical basis for TS in skin while sparing or minimizing this effect in bone as well as tendinoligamentous tissues. Based upon the possibility of subclinical expression of heterozygote phenotypes previously discussed (Abbas, 1999; Zhang, 2000; Tan, 2003; Khan, 2005; Hedrich, 2006; Dagda, 2009), the potential for altered Type I collagen organization in HERDA heterozygotes provides a rationale for investigating the role of the HERDA mutation in the increased prevalence of osteochondrosis lesions in cutting horses (Contino, 2012) as HERDA carriers are over-represented in elite performers (Tipton, 2008; equistat.com, Tryon, 2009).

This investigation identifies significantly lower TS of tendinoligamentous structures and EM of great vessels from horses with HERDA, providing the first evidence that the homozygous HERDA phenotype includes weakening of tissues that are not part of the integumentary covering of the body. We confirmed a previously reported (Grady, 2009) significant decrease in tensile properties of skin from corporal regions that are not on the dorsum of HERDA homozygotes and provide an explanation for the propensity to lesions along the dorsum in HERDA because the reduced strength of HERDA skin is more extreme at the withers relative to forelimb and abdominal skin. Accordingly, the

homozygous HERDA phenotype is not restricted to integumentary tissues, nor to dorsal regions of the skin, constituting a phenotype refinement that is relevant to investigating the role of CYPB in collagen metabolism and of the CYPB mutation in clinical HERDA. In the context of human patients that are heterozygous for PARKIN and PINK1 mutations and exhibit subtle manifestations of the associated homozygous Parkinson's phenotype (Abbas, 1999; Zhang, 2000; Tan, 2003; Valente, 2004; Khan, 2005; Hedrich, 2006; Dagda, 2009), the decreased TS of tendinoligamentous structures we observed in HERDA homozygotes highlight the relevance of quantifying biomechanical properties of tissues from HERDA carriers for attributes that could convey an advantage in disciplines requiring extremes of flexibility and lateral movement.

Table 2 Tensile values (Mean, 95% Confidence Interval) and fixed effect p-values of tissues from HERDA vs. control horses. (*significant at p<0.05)

	Mean, 95% Confidence Interval		P-values for Fixed Effects in Model		
	Control	**HERDA**	Disease Status	Location	Disease Status x Location Interaction
Tensile Strength (MPa)					
Skin			<0.001*	0.202	0.053
Withers	20.72, 7.30	3.97, 2.36*			
Forelimb	14.24, 4.99	6.21, 2.27*			
Abdomen	11.90, 7.21	5.09, 1.70			
Average	15.62, 3.99	5.09, 1.36*			
Vessels			0.092	0.018*	0.881
Aorta	0.45, 0.16	0.26, 0.05			
Pulmonic Artery	0.76, 0.34	0.54, 0.18			
Average	0.61, 0.16	0.40, 0.10			
Tendinoligaments			0.016*	<0.001*	0.577
SFT	111.32, 9.23	90.90, 15.66			
DFT	111.82, 9.23	101.64, 9.94			
SL	63.39, 12.15	49.89, 8.49			
Average	95.51, 12.15	80.81, 12.38*			
Elastic Modulus (MPa)					
Skin			<0.001*	0.489	0.968
Withers	48.89, 19.43	14.93, 4.42*			
Forelimb	56.81, 26.43	23.10, 8.16*			
Abdomen	48.07, 32.34	17.42, 5.43			
Average	51.26, 14.54	18.48, 2.55*			
Vessels			0.039*	0.006*	0.326
Aorta	0.90, 0.35	0.55, 0.13			
Pulmonic Artery	2.04, 0.87	1.18, 0.32			
Average	1.47, 0.46	0.86, 0.20*			
Energy to Failure (mJ/mm^3)					
Skin			0.001*	0.112*	0.055
Withers	4.99, 1.73	1.26, 1.07*			
Forelimb	3.85, 1.66	1.90, 0.66			
Abdomen	2.25, 0.98	1.54, 0.87			
Average	3.70, 0.97	1.56, 0.62*			
Vessels			0.174	0.079	0.487
Aorta	0.18, 0.08	0.09, 0.02			
Pulmonic Artery	0.22, 0.04	0.19, 0.09			
Average	0.20, 0.05	0.14, 0.04			

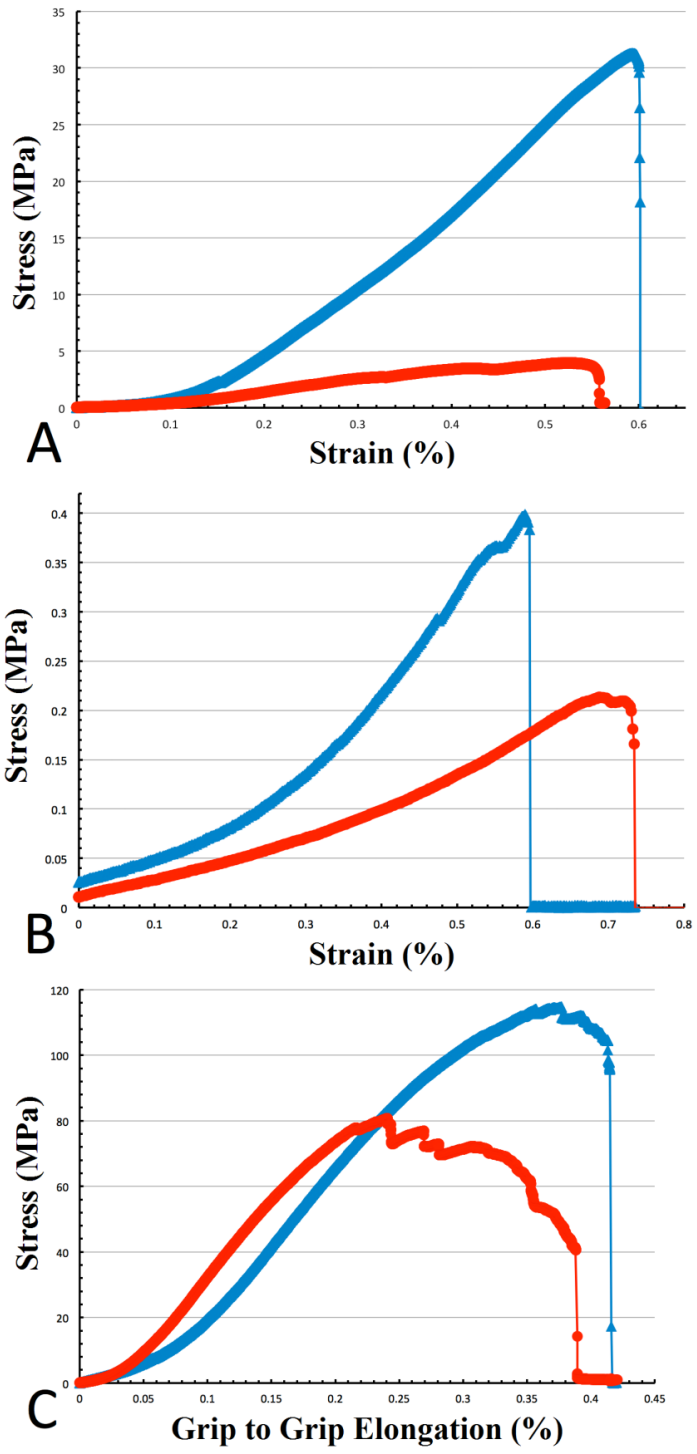

Figure 6 Representative Tissue Stress vs. Strain Curves.

A: skin (withers) and **B**: vessel (aorta), and stress vs. grip to grip elongation curve for **C**: Tendinologaments (SFT) of control (▲) versus HERDA (●) horses.

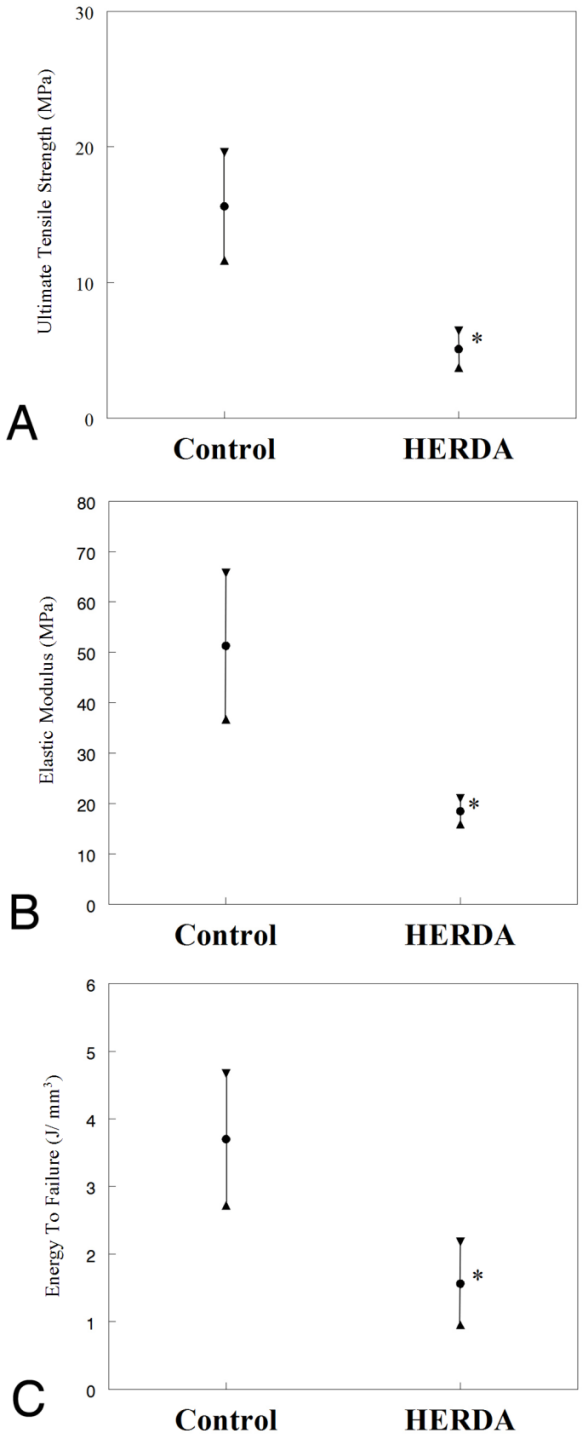

Figure 7 Tensile Properties of Control and HERDA Skin.

Data is represented as the mean (●) and 95% confidence interval (▼,▲) for TS (**A**), elastic modulus (**B**), and energy to failure (**C**) of control (n=18) and HERDA (n=18) skin. *p<0.001.

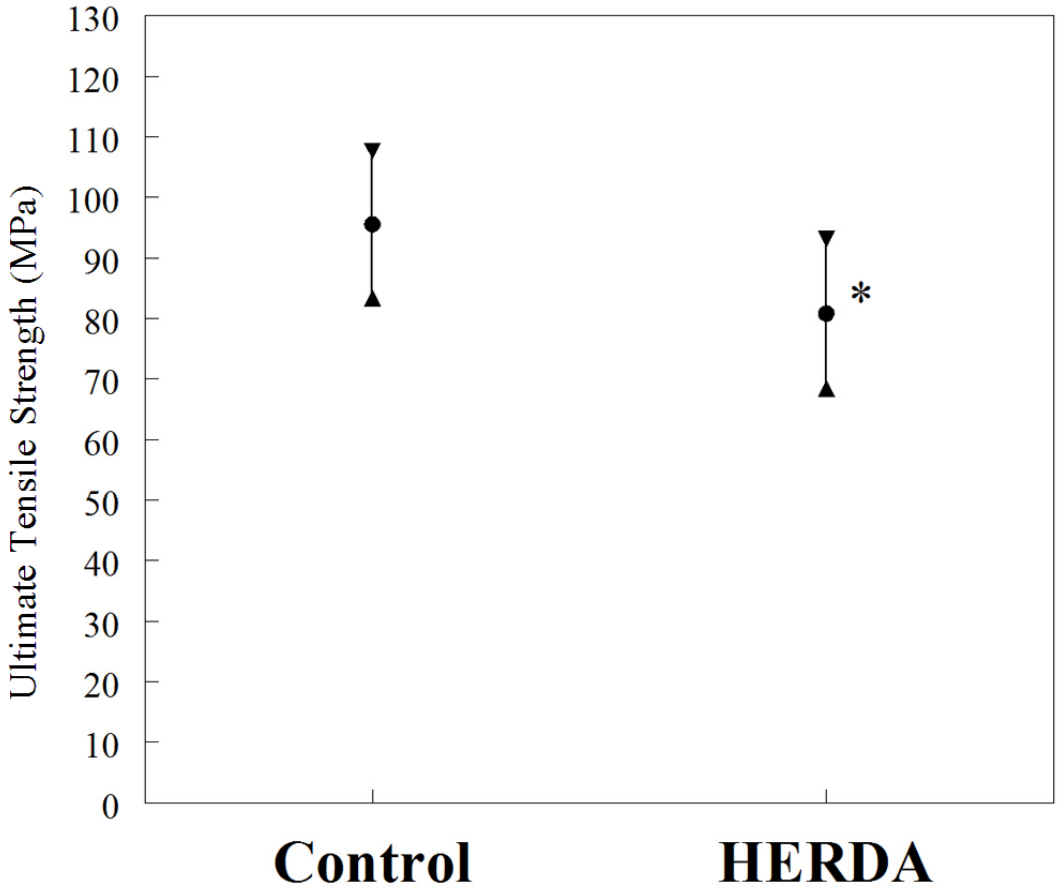

Figure 8 Tensile Strength Control and HERDA Tendinoligaments.

Data is represented as the mean (●) and 95% confidence interval (▼, ▲) for TS of control (n=18) and HERDA (n=18) tendinoligaments. *p=0.016.

CHAPTER IV

LYSYL HYDROXYLASE-1 AND CYCLOPHILIN-B INTERACTIONS: PROPOSED MECHANISM FOR ETIOPATHOGENESIS OF HEREDITARY EQUINE REGIONAL DERMAL ASTHENIA

Summary

Objective

The objective of this investigation was to identify the molecular mechanisms by which the HERDA mutation in the gene encoding Cyclophilin-B (PPIB) causes the clinical syndrome of skin fragility in HERDA Quarter Horses. Based upon prior investigations in our laboratory (Hill, 2010) that demonstrated decreased lysine hydroxylation and an associated increase in deoxypyridinoline in HERDA skin, we hypothesized that the HERDA PPIB mutation modifies an uncharacterized interaction between Cyclophilin B (CYPB) and Lysyl Hydroxylase-1 (LH1). This interferes with hydroxylysine synthesis and its availability for collagen crosslink formation. In addition, the HERDA PPIB mutation may also lead to modifications of other known CYPB protein complexes, such as the prolyl-3hydroxylase-1: cartilage associated protein: cyclophilin B triplex.

Methods

Two methods were used to identify the putative interaction between CYPB and LH1 and to identify modification of this interaction by the HERDA CYPB mutation. First, co-immunoprecipitation (Co-IP) was performed on liver tissue and cultured fibroblasts from both control and HERDA affected horses. Co-IP was instituted initially with antibody to CYPB followed by western blot analysis of the precipitate using anti-LH1. This method was also reversed such that Co-IP was performed using anti-LH-1 followed by western blot analysis using anti-CYPB. In situ interaction between CYPB and LH1 in HERDA homozygotes, heterozygotes, and horses lacking the HERDA allele was assessed in fibroblasts using proximity ligation assay (PLA). PLA was also used to assess interaction between prolyl-3 hydroxylase-1 (P3H1) and cartilage associated protein (CRTAP) in control and HERDA homozygous fibroblasts.

Study Results

Interaction between CYPB and LH1 was confirmed using PLA in equine fibroblasts. This CYPB-LH1 interaction was identified in fibroblasts from horses that were homozygous and heterozygous for the HERDA allele, as well in control horses that lack the HERDA allele. However, the relative quantity of the CYPB-LH1 interaction was reduced in both HERDA homozygotes and heterozygotes when compared to controls. Protein-protein interaction between P3H1 and CRTAP was also documented using PLA in fibroblasts from HERDA homozygotes and controls. In this experiment the degree of interaction was reduced in fibroblasts from HERDA homozygotes relative to controls without the HERDA allele.

Conclusion and Significance

These results substantiate our hypothesis that a protein-protein interaction occurs between CYPB and LH1 during collagen processing. Counter to findings in a prior investigation (Ishikawa, 2012), these results also indicate that the CYPB-LH1 interaction does occur in fibroblasts containing either one or two copies of the mutant HERDA PPIB allele but this interaction is attenuated in the presence of the HERDA CYPB mutation. In addition, interactions between P3H1 and CRTAP were also attenuated in cells homozygous for the PPIB mutation. In light of our prior evidence of decreased lysine hydroxylation and altered collagen cross-linking in HERDA skin, this information refines the mechanistic link between the HERDA PPIB mutation and the disease phenotype of fragile hyper-extensible skin. Our prior finding (Hill, 2010) of decreased hydroxylysine concentrations in collagen from HERDA homozygotes suggests that interactions between CYPB and LH1 are necessary for proper post-translational hydroxylation of lysine residues in procollagen. Decreased hydroxylysine availability as a substrate for intermolecular collagen crosslinking would decrease collagen tensile strength and modifying elasticity consistent with our findings in tissues with high fibrillar collagen content (Bowser, 2012). In addition, the evidence of decreased interaction between CYPB and LH1 in cells from HERDA heterozygotes represents a quantifiable phenotype in animals with a single copy of the PPIB mutation. This provides a mechanistic basis from which to investigate the link between heterozygosity for the HERDA allele and a performance advantage in the western performance discipline of cutting (Tipton, 2008; equistat.com).

Introduction

Hereditary equine regional dermal asthenia (HERDA), also known as hyperelastosis cutis (HC) is an autosomal recessive genetic disease of Quarter Horses and related breeds that is characterized by fragile skin that is velvety in texture, loose and hyper-extensible (Lerner, 1978; Hardy, 1988; Pascoe, 1999; Stannard, 2000; White, 2004, 2007). The proposed causal mutation, a c.115G>A missense mutation in the gene encoding Cyclophilin B (PPIB) has to date been found to segregate in concordance with symptomatic horses and known inbreeding loops for heterozygosity (Tryon, 2007, 2009; Ishikawa, 2012). A member of the peptidyl-proplyl isomerase family of proteins, CYPB executes certain essential chaperoning functions during fibrillogenesis (Kozlov, 2010; Zhang, 2003; Smith, 1995; Horibe, 2002; Meunier, 2002). These functions include cis-trans isomerization of peptidyl-prolyl bonds in procollagen chains, thus catalyzing collagen triple helix formation (Bachinger, 1987; Liu, 1990; Smith, 1995; Kanty, 2005; Pyott, 2011). In addition, CYPB complexed with prolyl 3-hydroxylase 1 (P3H1) and cartilage associated-protein (CRTAP) act together to catalyze hydroxylation of proline residues at position 986 of the α1 chains of type I, II, and III collagen (Ishikawa, 2009). Mutations in any of these 3 proteins decreases Pro-986 hydroxylation and are among the causes of severe to lethal recessive osteogenesis imperfecta (OI) (Van Dik, 2009; Choi, 2009; Barnes, 2010; Vranka, 2010; Pyott, 2011).

Recently, it was found that the HERDA mutated CYPB retains cis-trans isomerization activity, but shows delayed collagen folding and secretion (Ishikawa, 2012) without over-hydroxylation of lysine residues, a phenomenon termed over modification that is typically associated with delayed collagen secretion (Willing, 1988; Cabral, 2007;

Christiansen, 2010). The region on the CYPB protein altered by the HERDA mutation is not associated with cis-trans isomerization catalysis, but with identification of improperly folded proteins in the endoplasmic reticulum (Kozlov, 2010) and lysyl hydroxylase-1(LH1) association (Ishikawa, 2012). Furthermore, analysis of Pro-986 hydroxylation in type I collagen yielded only minor changes in HERDA versus control skin and tendons (Ishikawa, 2012).

Clinically similar connective tissue dysplasias of both autosomal recessive and dominant natures have been documented in a wide array of mammalian species such as cats, dogs, cattle, sheep, rabbits, mice and man (Arlein, 1947; Minor, 1983; Holbrook, 1980; Sequeira, 1999; Tajima, 1999; van Halderen, 1988; Brown, 1993; Harvey, 1990; Choi, 2009). Ehlers-Danlos syndromes (EDS) are a heterogenous group of inherited connective tissue disorders in people where skin hyperextensibility and tissue fragility closely resemble the HERDA phenotype (Lerner, 1978; Hardy, 1988; Brounts, 2001; White, 2004). EDS VIA is an autosomal recessive disorder of LH1 activity (Yeowell, 2000; Uzawa, 2003), which is responsible for hydroxylation of lysine residues in procollagen peptides (Valtavaara, 1997; Myllylä, 1998). EDS VIA individuals have significantly decreased procollagen hydroxylysine residues which are essential for formation of covalent pyridinium crosslinks in Type I collagen (Mao, 2001; Fernandes, 2008). Furthermore, the ratio between the 2 most common pyridinium crosslinks, deoxypyridinoline (DPD): pyridinoline (PYD) is greatly increased, which is currently used for diagnosis of this condition (Pasquali, 1994; Mao, 2001; Fernandes, 2008). Affected HERDA horses also exhibit both reduced total hydroxylysine in skin and the increased ratio of DPD: PYD in both skin and urine, (Swiderski, 2006; Hill, 2010) while

having normal LH1 activity and sequence (Pasquali, Bayrak-Toydemir, unpublished). Ishikawa recently demonstrated that recombinant equine (wild type) CYPB expressed in E. coli binds to LH1 in rough endoplasmic reticulum (rER) extract from chick embryos, but this binding did not occur in the presence of similarly expressed recombinant HERDA CYPB (Ishikawa, 2012). Collectively our findings substantiate a novel interaction between Cyclophilin B and LH1 which is modified by the HERDA PPIB mutation.

The objective of this study was to first document the presence of binding between CYPB and LH1 in horse fibroblast cell lines and to evaluate differences in the degree of this CyPB-LH1 interaction within HERDA homozygous, heterozygous and control animals. In addition, we sought to also measure the degree of interaction between P3H1 and CRTAP in HERDA homozygous and control horses.

Materials and Methods

Samples

Sample collection and use in this investigation was approved by the Institutional Animal Care and Use Committee (IACUC). Disease status of all samples was confirmed via HERDA genotyping by Dr. Nena Winand, Cornell University Diagnostic Laboratory[d] or the Veterinary Genetics Laboratory, University of California, Davis[h].

Liver Tissue Collection

Liver tissues were harvested from control and HERDA homozygous horses following humane euthanasia at the Mississippi State University College of Veterinary

Medicine. Samples were collected within 2 hours of euthanasia, placed into evacuated whirl paks (Nasco[e], Cat# B00679WA), and stored at -80°C until assayed.

Fibroblast Cultures

Skin fibroblast cultures from control and HERDA homozygous horses were prepared from dermal punch biopsies collected antemortem using aseptic conditions or from skin collected immediately post mortem. The skin was minced in Dulbecco's phosphate buffered saline (DPBS) containing 200 µg/ml penicillin/streptomycin (Sigma-Aldrich[i], Cat# P433). Minced tissue fragments were resuspended in fibroblast media (Dulbecco's Modified Eagle's Medium/Nutrient Mixture F-12 Ham media (Sigma-Aldrich[i], Cat# D6421) containing 20% fetal bovine serum (FBS) (Gemini Bio-Products[j], Cat# 100-106), 100 µg/ml penicillin/streptomycin (Sigma-Aldrich[i], Cat# P433) and 2mM L-glutamine (Sigma-Aldrich[i], Cat# G7513), and plated in 6 well plates that were precoated with fibronectin coating mix (Athena Enzyme Systems[k], Cat# 0407). Cells were incubated at 37°C in atmosphere supplemented to 5% CO_2, monitored for outgrowth and passaged serially from 25cm^2 to 50cm^2 flasks. At 70% confluence, cells were rinsed 3 times in DPBS, detached from flasks via trypsinization and centrifuged at 1000 rpm for 10 minutes. Cells were counted and 2- 2.5 x 10^6 cell aliquots were resuspended in media with 20% FBS. DMSO (Sigma-Aldrich[i], Cat# 472301) was added dropwise to achieve a 10% solution. Aliquots were then placed in an isopropyl alcohol cell freezer designed to assure proper freezing of eukaryotic cells to -80oC at 1oC per minute (Mr Frosty, Thermo Scientific[l], Cat# 5100-0001), placed at -80°C overnight, and transferred to cryopreservervation (-256°C).

For experiments evaluating collagen metabolism, cells were defrosted at room temperature, and cultured in 25cm^2 flasks in fibroblast media at 37°C in 5% CO_2. At 90% confluence cells were transferred to single well (~110 cm^2) plates (Thermo Scientific[l], Cat# 165218). Growth was monitored until ~80 % confluence and then 50µg/ml ascorbic acid (Sigma-Aldrich[i], Cat# A4403) was added to the media 18 hrs prior to harvesting. At collection, cells were washed three times with DPBS and scraped into 1.5ml microcentrifuge tubes, pulse centrifuged to produce a cell pellet, and supernatant discarded. Cell pellets (approximately ~10^8cells) were stored @ -20°C until assayed.

Fibroblast Lysate Preparation

Immediately prior to assay, one, two, four or eight previously collected cell pellets from each cell line were thawed, and lysed in NP40 Cell Lysis Buffer (Invitrogen[m], Cat #FNN0021) containing protease inhibitor (Sigma-Aldrich[i], Cat# P2714) via 30 minute incubation on ice with vortexing every 10 minutes. Samples were centrifuged at 10,000rpm x 10min at 4° C and the pellet discarded.

Endoplasmic Reticulum Enriched and Purified Lysate Preparation

Endoplasmic reticulum enriched and purified post mitochondrial fraction (ER-PMF) lysates were obtained from both cultured fibroblasts and liver tissue using the ER Isolation Kit (Sigma-Aldrich[i], Cat# ER0100-1KT).

Fibroblast ER-PMF

Fibroblast cell pellets (~10^8 cells/pellet) previously described were thawed, re-suspended in a volume of 1X Hypotonic Extraction Buffer (Sigma-Aldrich[i]) equivalent to 3 times the cell pellet packed cell volume (PCV) and incubated for 20 minutes at 4°C.

Subsequently, the cells were centrifuged at 600 x g for 5 minutes and the supernatant was removed by aspiration. PCV was again measured and a volume of 1X Isotonic Extraction Buffer (Sigma-Aldrich[i]) equivalent to 2 times the new PCV was added. The mixture was sheared through a 23 gauge needle with a 5 mL syringe 3-5 times to produce a homogenate.

The homogenate was maintained on ice and centrifuged at 1000 x g for 10 minutes at 4°C. The thin floating lipid layer was carefully aspirated and the post nuclear supernatant was pipetted into a clean microfuge tube and pellet discarded. The supernatant was centrifuged at 12000 x g for 15 minutes at 4°C and lipid layer carefully removed by aspiration again. The clear post nuclear supernatant ER-PMF was transferred into another clean microcentrifuge tube and pellet discarded. Proteins in the post nuclear supernatant ER-PMF were precipitated by adding 7.5 volumes of 8mM Calcium Chloride Solution (Sigma-Aldrich[i]) dropwise with constant stirring. The solution was stirred for an additional 15 minutes at 4°C and centrifuged at 8000 x g for 10 minutes. The pellet was resuspended in 0.3 mL of 1X Isotonic Extraction Buffer (Sigma-Aldrich[i]) for subsequent use in the co-immunoprecipitation assay described below.

Liver ER-PMF

Liver tissue samples (1 g per assay) were sliced into 2mm pieces, rinsed twice in DPBS, blotted to remove excess blood contamination and pulverized by passage through a stainless steel wire mesh with glass homogenizer and 1X Isotonic Extraction Buffer (3.5mL/g tissue). The homogenate was then processed identically to the fibroblast homogenate described previously to produce a hepatocyte ER-PMF.

Co-Immunoprecipitation

Protein content of the ER fractions (fibroblast and hepatocyte ER-PMF) were estimated by diode array spectrophotometer (NanoDrop 2000, Thermo Scientific[l]) and protein quantity standardized between samples before proceeding to Co-immunoprecipitation (Co-IP). A protein G magnetic bead kit (Dynabeads, Invitrogen[m], Cat# 100.07D) was used in all Co-IP reactions according to product instructions. Protein G coated magnetic beads were prepared by 60 minute incubation with 2 µg primary antibody in 200µl antibody binding and washing buffer (Invitrogen[m]). Primary antibodies were either rabbit origin polyclonal anti-CYPB (Abcam[q], Cat# ab16045) for the forward assay (Co-IP using anti-CYPB with detection of LH1 by western blot), or goat origin polyclonal anti-LH1 (Santa Cruz Biotechnology[n], Cat# sc-50063) for the reciprocal assay (Co-IP using anti-LH1 with detection of CYPB by western blot). To minimize antibody dissociation from the beads, primary antibody was crosslinked to the magnetic beads using bis[sulfosuccinimidyl] suberate (BS^3, Thermo Scientific[l], Cat# 21586) at a 10 fold molar excess to the primary antibody. Following incubation at room temperature for 30 minutes, the crosslinking reaction was quenched using Tris at a final concentration of 40mM for 15 minutes. Protein G coated magnetic beads with crosslinked anti-CYPB were washed three times with 200µl phosphate buffered saline with Tween 20 (PBST) and separated from the supernatant using a magnet.

Anti-CYPB coated magnetic beads were incubated with the prepared cell lysates for 60 minutes at room temperature with rotation and gentle pipetting. Beads were separated from the supernatant with a magnet, washed 3 times using 200µl washing buffer (Invitrogen[m]) per sample, resuspended in 100µl washing buffer and transferred to

1.5ml microcentrifuge tubes. Proteins were eluted from the magnetic beads by adding 40µl elution buffer (Invitrogen[m]), 20µl NuPAGE LDS Sample Buffer (Invitrogen[m]) and incubating at 95°C for 10 minutes.

Polyacrylamide Gel Electrophoresis

Following elution and heating, samples from Co-IP were immediately quenched on ice and pulse centrifuged prior to loading onto precast polyacrylamide gels (Criterion TGX-Any kD, Bio-Rad[o], Cat# 567-1123). Gels were run in duplicate by loading half of the eluted Co-IP product (by volume) to produce 2 identical gels. Control lanes on each gel included recombinant Human CYPB protein (ProSpec-Tany TechnoGene[p], Cat# ENZ-313), rabbit origin polyclonal anti-CYPB Antibody (Abcam[q], Cat# ab16045), mouse ovarian extract as an LH1 control (Santa Cruz Biotechnology[n], Cat#.sc-2404). A protein molecular weight standard was incorporated in the outer flanking wells (Magic Mark, Invitrogen[m], Cat# LC5603). Proteins were resolved by electrophoresis at 4°C overnight in 1X NuPAGE MES SDS running buffer (Invitrogen[m], Cat# NP0002).

Early in the protocol, one of the duplicate gels was stained with silver stain (Pierce[r], Cat# 24600). Later, due to concerns about silver interference with mass spectrometry analysis, the duplicate gel was stained with GelCode Blue (Thermo Scientific[l], Cat# 24590). Silver staining was conducted per kit protocol directions. GelCode Blue stain, a modified coomasie dye with increased protein detection sensitivity above traditional coumassie blue staining (sensitivity approaching 8 nanograms), was used per kit protocol instructions.

LH1 is a homodimer. Consistent with ER fraction proteins, the predicted sequence for equine LH1 (NCBI-GI: 149695386) in the absence of post-translational

modification would migrate in the range of 84 kD. Human LH1 is estimated to migrate at 85kD (Valtavaara, 1997). Human CYPB monomer has a predicted molecular mass of 21kD (Endrich, 1999) and equine CYPB (NCBI- GI:153792483), in the absence of post-translational modification has a predicted molecular mass of 23.563 kD. Following staining, bands visible in these regions were cut from the gel and frozen at -80°C for later analysis.

Western Blot Analysis

Following gel electrophoresis of immunoprecipitated proteins, one of the duplicate polyacrylamide gels was immediately transferred to polyvinylidene difluoride (PVDF) membrane (Bio-Rad[o], Cat# 162-0236) by electrophoresis at 60 volts for 90 min. The membrane containing transferred protein was subjected to modified western blot (Sambrook, 2001). Briefly, the membrane was blocked overnight at 4°C with 5% bovine casein (Bio-Rad[o], Cat# 170-6404), incubated one hour with either goat origin anti-LH1 (Santa Cruz Biotechnology[n], Cat# sc-50063) or rabbit origin anti-CYPB (Abcam[q], Cat# ab16045) and washed four times for 5 minutes with Tris-Tween Buffered Saline (TTBS). The membrane was then incubated 1 hour with either donkey anti-goat IgG-HRP (Santa Cruz Biotechnology[n], Cat# sc-2020) for to detect LH1, or goat anti-rabbit IgG-HRP (Santa Cruz Biotechnology[n], Cat# sc-2004) to detect CYPB. The membrane was washed 4 times (5 minutes per wash with TTBS), incubated for 5 minutes with horseradish peroxidase enhanced chemiluminescence solution (Pierce[r], Cat# 34087) and imaged on a Bio-Rad ChemiDoc XRS+ System (Bio-Rad[o]).

Proximity Ligation Assay

Fibroblast Preparation

Skin fibroblast cultures from control, HERDA heterozygous and homozygous horses were prepared from skin biopsies as previously described. Cells were plated into 12-well plates containing 10mm diameter glass coverslips and grown in AmnioMAX media (Invitrogen[m], Cat# 11269-016) containing Alpha-MEM Earle's Salts (Irvine Scientific[s], Cat# 9144), 20% fetal bovine serum (Gemini Bio-Products[j], Cat# 100-106), 100 µg/ml penicillin/streptomycin (Sigma-Aldrich[i], Cat# P433) and 2mM L-glutamine (Sigma-Aldrich[i],Cat# G7513) and allowed to attach overnight. Cells were incubated in the presence of ascorbic acid (50µg/ml) (Sigma-Aldrich[i], Cat# A4403) for 18 hours prior to use in the immunofluorescence or proximity ligation assays.

Immunofluorescence

Immunofluorescence was performed using a modified protocol from Abcam. Briefly, fibroblast cells as described previously were rinsed with cold 1× phosphate buffered saline (PBS), fixed with 4% paraformaldehyde in 1× Sorenson's solution (Abcam[q]) for 15 minutes at room temperature and permeabilized with 0.25% Triton X-100 in 1× PBS at room temperature for 12 minutes. Following a 1 hour blocking treatment in either 2% goat serum (Zymed[t], Cat# 10000C) for cells to be incubated with anti-CRTAP, anti-P3H1, or anti-CYPB; or Duolink block solution (Olink[u]) for cells to be incubated with anti-LH1 at room temperature, primary antibodies to CYPB (Abcam[q], Cat# ab16045), LH1 (Santa Cruz Biotechnology[n], Cat# sc-50063), CRTAP (Morello[v]) or P3H1 (Abnova[w], Cat# H00064175-B01P) were added in separate wells and allowed to hybridize at room temperature for two hours. Secondary antibodies conjugated to

fluorophores (Jackson Laboratories[x], Cat# 111-075-144, 705-095-147): goat anti-rabbit TRED (1:400), donkey anti-goat FITC (1:200); (Molecular Probes[y], Cat# A11008, A11032): goat anti-rabbit Alexa Fluor 488 (1:800), goat anti-mouse Alexa Fluor 594 (1:800) were then incubated with cells as appropriate for the primary antibody at room temperature for one hour. Coverslips were mounted on glass slides with 4′, 6-diamidino-2-phenylindole (DAPI) (Prolong +, Invitrogen[m], Cat# P36935). Cells were visualized microscopically using fluorescence detection (Nikon microphot-SA microscope, Nikon Instruments[z]) and digitally imaged(Photometrics sensys, Photometrics[aa]).

Proximity Ligation

The Duolink in situ Proximity Ligation Assay (PLA, Olink Bioscience[u]) was used to detect interactions between CYPB and LH1, and also between CRTAP and P3H1. The Duolink system employs oligonucleotide-labeled secondary antibodies (PLUS and MINUS probes with complementary DNA sequences) to each of the primary antibodies (CYPB and LH1 or CRTAP and P3H1) that, in combination with a DNA amplification-based reporter system, generate a fluorescent signal only when the two primary antibodies are in close proximity (Wilhelm, 2010). Signal from a single pair of primary antibodies is visualized as a fluorescent spot (see Figure 9 for an overview of the PLA method).

Briefly, fibroblasts were cultured *in vitro*, fixed, permeabilized and blocked with Duolink block solution as previously described for immunofluorescence. PLA was performed as per manufacturer's instructions. Antibodies for both CYPB (1:100) and LH1 (1:100), or both CRTAP (1:2000) and P3H1 (1:4000) were added to each well and incubated for 1hour 40 minutes. Coverslips were washed with 1× PBS and incubated

with PLA probe solution (Olink[u]) containing PLUS and MINUS probes in a humidity chamber at 37° C for one hour, washed again, and incubated with Duolink Ligase-Ligase solution (Olink[u]) for 30 minutes in the same conditions as the previous step. Coverslips were washed using Duolink 1X Wash Buffer A (Olink[u]) and incubated with polymerase containing amplification solution (Olink[u]) in a humidity chamber at 37° C for 1 hour 40 minutes. Finally, the cells were washed using Duolink Wash Buffer B (Olink[u]) in decreasing concentration (1X, then 0.01X), coverslips were allowed to dry and mounted in Duolink II Mounting Media (Olink[u]) with DAPI (Invitrogen[m], Cat# P36935). Images were captured as described previously.

Results of Study

Co-Immunoprecipitation

Silver stained gels produced by forward (anti-CYPB) immunoprecipitation of fibroblast lysate from 1, 2, 4 or 8 cell pellets produced no or equivocal discernible bands at ~85kD where LH1 migration is anticipated. Silver stained gels produced by reciprocal (anti-LH1) immunoprecipitation of increasing fibroblast lysate concentrations also failed to demonstrate appropriate 21kD bands congruent with CYPB pull-down. Use of increasing numbers of cells enhanced non-specific binding during the Co-IP procedure and increased background signal in the western blot analysis. Neither LH1 nor CYPB were identified by western blot analysis from Co-IP of non-ER enriched fibroblast lysates.

Silver stained gels produced by forward (anti-CYPB) immunoprecipitation of ER enriched fibroblast lysate demonstrated faint bands of ~85kD suggestive of LH1 pull-

down. However, western blot of this anti-CYPB derived Co-IP product to identify LH1 was negative or equivocal.

Silver stained gels produced by anti-CYPB initiated immunoprecipitation of ER enriched and purified hepatocyte lysate produced moderate bands of correct ~85kD weight appropriate for LH1 pull-down (Figure 10). Furthermore, western blot analysis of these assays produced some positive LH1 signal (Figure 11). Unfortunately, mass spectrometry of these fragments failed to confirm them as LH1. Following this, subsequent gels produced from immunoprecipitation of ER enriched and purified hepatocyte lysate were stained using a coomassie blue (GelCode Blue, Pierce[r]) based staining method in order to minimize interference with mass spectrometry analysis. Appropriate bands visualized using this staining technique were fainter, but still visible. Again mass spectrometry analysis failed to confirm the bands as LH1.

Proximity Ligation

Immunofluorescence assays using control fibroblasts confirmed good intracellular staining by the CYPB, LH1, CRTAP and P3H1 primary antibodies (Figure 12) for use in subsequent PLA procedures. Furthermore, these proteins appeared to concentrate in a peri-nuclear pattern appropriate for residing in the endoplasmic reticulum.

CYPB-LH1 Interaction

Positive interaction between CYPB and LH1 was found via PLA in equine fibroblasts homozygous, heterozygous and lacking the HERDA PPIB mutation (Figure 13). Total relative quantity of individual CYPB-LH1 complexes (fluorescent spots) was reduced in HERDA homozygotes and heterozygotes when compared to controls. The

total quantity of individual CYPB-LH1 complexes in both heterozygote and homozygote fibroblasts appeared to be roughly 50% reduced from control fibroblasts lacking the HERDA allele. Quantitative analysis of differences in protein-protein interactions necessitates analysis with proprietary software.

CRTAP-P3H1 Interaction

Positive interaction between P3H1 and CRTAP was found using PLA in equine fibroblasts homozygous for the HERDA PPIB mutation and lacking the mutation (Figure 14). Relative to the quantity of CRTAP-P3H1 interactions detected in control fibroblasts, CRTAP-P3H1 interactions were reduced in HERDA homozygote cells. The total quantity of individual CRTAP-P3H1 interactions in HERDA homozygous fibroblasts was roughly 70% reduced from control fibroblasts without the HERDA allel. Quantitative analysis of differences in CRTAP-P3H1 complex formation associated with the HERDA mutation necessitates software analysis.

Discussion

Procollagen chain modification, assembly and secretion from the endoplasmic reticulum is a complex and incompletely understood biological process that necessitates the coordinated interaction of many proteins (Gunson, 1979; Liu, 1990; Zhang, 2003; Canty, 2005; Krane, 2008; Fratzel, 2008). Recent advances in our understanding of the intricacies of these interactions (Choi, 2009; van Dik, 2009; Barnes, 2010; Ishikawa, 2009, 2011; Pyott, 2011) have led to a new depth of insight into the multiple orchestrated protein-protein interactions needed to catalyze these events. A member of the peptidyl-proplyl isomerase family of proteins, CYPB is known to 1) trans isomerize (Xaa-Pro)

peptide bonds from the cis- configuration (Bachinger, 1987; Liu, 1990; Smith, 1995; Kanty, 2005; Pyott, 2011), 2) chaperone HSP47 for proper stabilization of the collagen triple-helix within the rER(Smith, 1995) and 3) create a triplex along with P3H1and CRTAP for 3-hydroxylation of Pro986 on α1(I) and Pro707 on α2(I) chains (Ishikawa, 2009). As a member of the family of 2-oxoglutarate dioxygenases, LH1 catalyzes the hydroxylation of lysine residues in X-Lys-Gly triplets (Valtavaara, 1997; Myllylä, 1998). In this study we have successfully documented by PLA that CYPB and LH1, previously known to act separately, in fact act in close association with each other within the endoplasmic reticulum of fibroblasts.

Duolink PLA is a highly sensitive, highly specific in-situ method for detection and visualization of interactions at the single molecule-molecule level (Wilhelm, 2010). This procedure is often sensitive enough to detect weak associations that cannot withstand more rigorous purification methods and can identify protein associations within the more natural environment of a cell, preserving the un-denatured conformation of the protein and better reflecting in-vivo molecular relationships. In contrast, co-immunoprecipitation produces best results from strong, robust and numerously occurring protein-protein interactions. We suspect that the action of CYPB in association with LH1 is of a chaperoning nature, similar to previously documented CYPB functions (Smith, 1995; Ishikawa, 2009), making the association between these two molecules transient and reversible. Failure to substantiate CYPB-LH1 interaction by the use of co-immunoprecipitation methods in our study is likely due to limited frequency and strength of the CYPB-LH1 interaction that occur under natural circumstances within the rER. Recently, a CYPB-LH1 interaction by modified immunoprecipitation technique was

successful documented using E. coli recombinant sepharose bead-bound equine CYPB incubated with rER extract from chick embryos (Ishikawa, 2012). It is possible that this technique helped to optimize both the amount of bead-bound CYPB and the quantity of LH1 available for CYPB binding to produce positive western blot pull-down results that were not apparent in the current study using more natural biologic concentrations found within fibroblast or hepatocyte lysates. Furthermore, in Ishikawa et al. (2012), recombinant HERDA mutated CYPB failed to bind LH1. This is in contrast to results in the current study documenting attenuated, but still present CYPB-LH1 binding *in-situ* within fibroblasts heterozygous and homozygous for the HERDA PPIB mutation. The increased sensitivity of Duolink PLA protein-protein detection is a plausible explanation for our ability to detect reduced, but present CYPB-LH1 binding within the present study.

The attenuation of CYPB-LH1 interactions within HERDA individuals found in this study helps to explain why these animals have reduced lysyl hydroxylation (Hill, 2010) despite normal LH1activity and sequencing (Pasquali, Bayrak-Toydemir, unpublished). In fact, delayed collagen folding and secretion in other diseases leads to procollagen over modification (Willing, 1988; Cabral, 2007; Christiansen, 2010) and increases total lysyl hydroxylation (Pasquali, 1997; Yeowell, 2000; Walker, 2004). Lysyl hydroxylation is reduced in HERDA individuals despite the presence of delayed collagen folding, a phenomenon that could not be explained prior to documentation of CYPB-LH1 interaction. The mutant HERDA CYPB attenuates CYPB-LH1 interaction, a step we hypothesize to be essential for optimal lysyl hydroxylation of lysine to hydroxylysine residues on the triple helical region of procollagen chains. This reduction in total hydroxylysine residues (Hill, 2010) leads to the preferential formation of the covalent

pyridinium crosslink, deoxypyridinoline (DPD), which is derived from less hydroxylysine residues (two hydroxylysines and one lysine) compared to pyridinoline (PYD), formally derived from 3 hydroxylysine residues. In the presence of unaltered CYPB, PYD is the most prevalent of the crosslinks, reflecting normal hydroxylation of both telopeptide and triple helical regions of collagen. The preferential formation of DPD observed in HERDA results in reversal of the DPD:PYD ratio in these horses (Hill, 2010), a phenomenon that is also documented in human patients with EDS VIA and impaired LH1 function (Beighton, 1997; Mao, 2001; Fernandes, 2008).

The finding that interaction between CRTAP and P3H1 is attenuated in HERDA homozygous fibroblasts is unexpected and interesting. CYPB participates in a collagen-modifying complex with CRTAP and P3H1, which together hydroxylate the proline at position 986 (P986) in the α1 chains of type I and type II collagens (Ishikawa, 2009). It is not surprising that the HERDA CYPB mutation alters optimal interaction between CRTAP and P3H1 in situ. Interestingly, mutations of any of these 3 components inhibits or impedes P986 hydroxylation and causes severe or lethal autosomal recessive osteogenesis imperfecta (OI) (Marini, 2007; Cabral, 2007; Choi, 2009; Vranka, 2010). OI is a disorder characterized by osteoporosis, bone fragility, and fractures that may be accompanied by bone deformity, tooth malformations, short stature, and shortened life span (King, 1971). Bone fragility has not been demonstrated in HERDA affected horses. Furthermore, analysis of Pro-986 hydroxylation in type I collagen yielded only minor changes in HERDA versus control skin and tendons (Ishikawa, 2012). Further investigation into the effect of attenuated CRTAP: P3H1 interaction of HERDA homozygotes on bone formation is warranted.

This study, to our knowledge, is the first documentation of altered protein-protein interaction in animals heterozygous for the HERDA allele. Previously, alterations in the tensile properties of connective tissues of HERDA affected animals have led us to hypothesize that carrier animals might also have altered (to a less extent) tensile properties of these structures (Bowser, 2012) which may provide an athletic advantage in competition. Attenuation of the CYPB: LH1 interaction in fibroblasts from HERDA heterozygotes provides evidence to advance the hypothesis that modified CYPB-LH1 interaction in HERDA carriers alters tissue biomechanical properties and accounts for the observed athletic advantage.

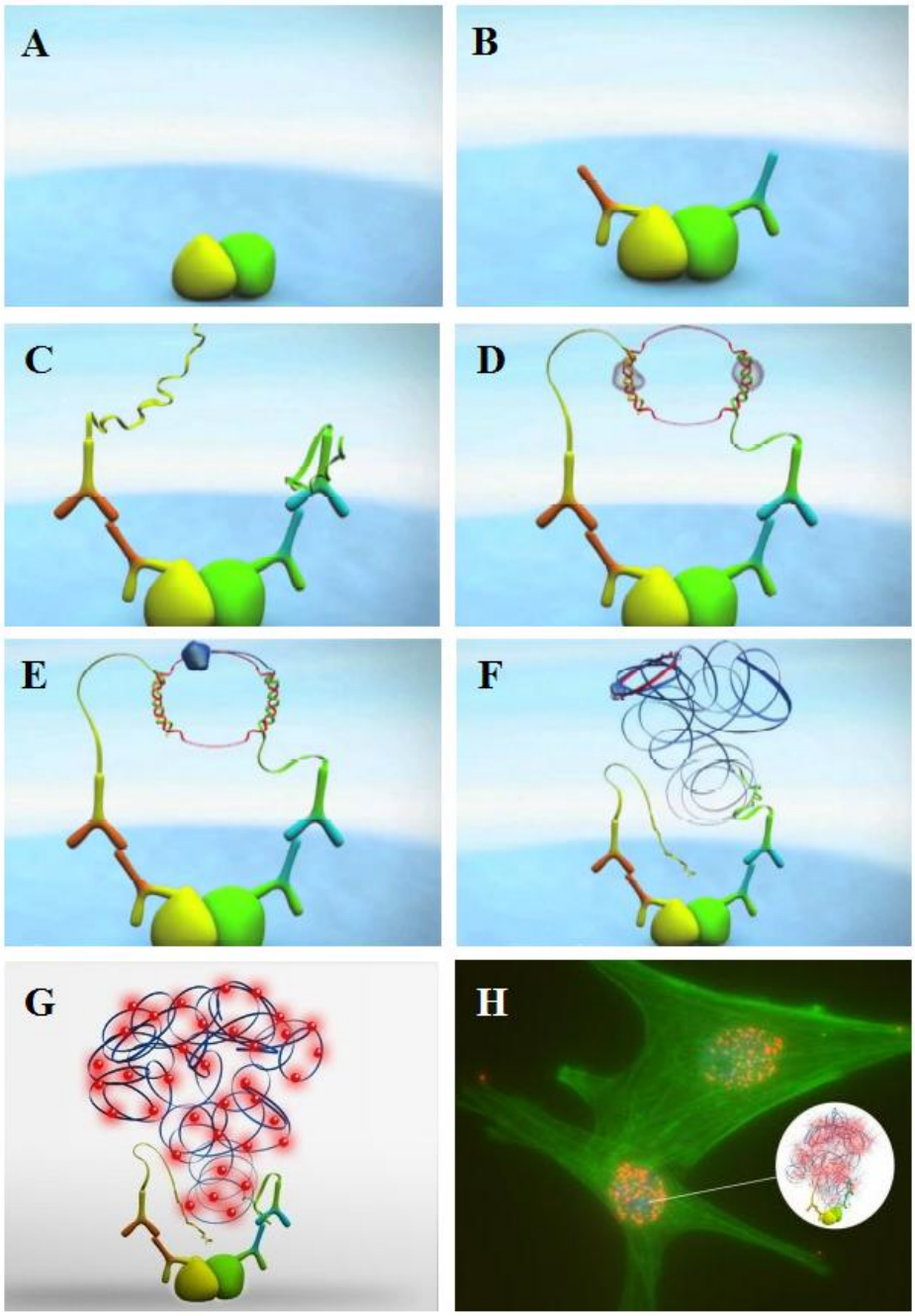

Figure 9 Overview of the Duolink Proximity Ligation Assay.

A) Two proteins interacting *in-situ*. B) Target specific primary antibodies of two different species. C) Oligonucleotide-labeled secondary antibodies (PLUS and MINUS probes). D) Oligos connector hybridization and ligation. E and F) Rolling circle amplification. G) Hybridization of detection probes. H) Visualization of each protein-protein complex as a single fluorescent spot.

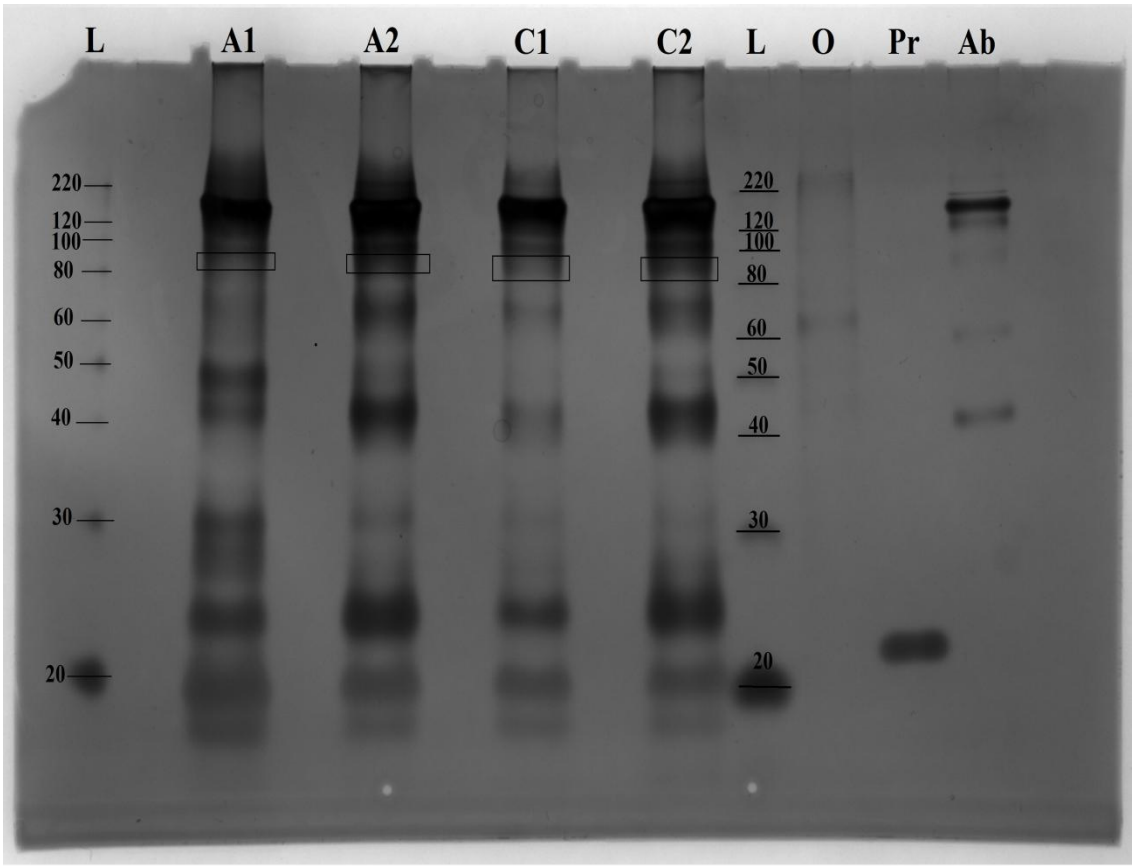

Figure 10 Anti-Cyclophilin B Co-immunoprecipitates from Endoplasmic Reticulum-Enriched Hepatocyte Lysates: Silver Stained Polyacrylamide Gel.

L: Protein standards. Values in kilodaltons (kD).
A1: HERDA homozygote 1, Anti-CYPB immunoprecipitate.
A2: HERDA homozygote 2, Anti-CYPB immunoprecipitate.
C1: Control 1, Anti-CYPB immunoprecipitate.
C2: Control 2, Anti-CYPB immunoprecipitate.
O: Mouse Ovarian Cell Lysate (LH1 positive control).
Pr: CYPB purified protein (CYPB positive control).
Ab: Anti-CYPB antibody.
Faint bands are visible (□) at approximately 85kD molecular weight.

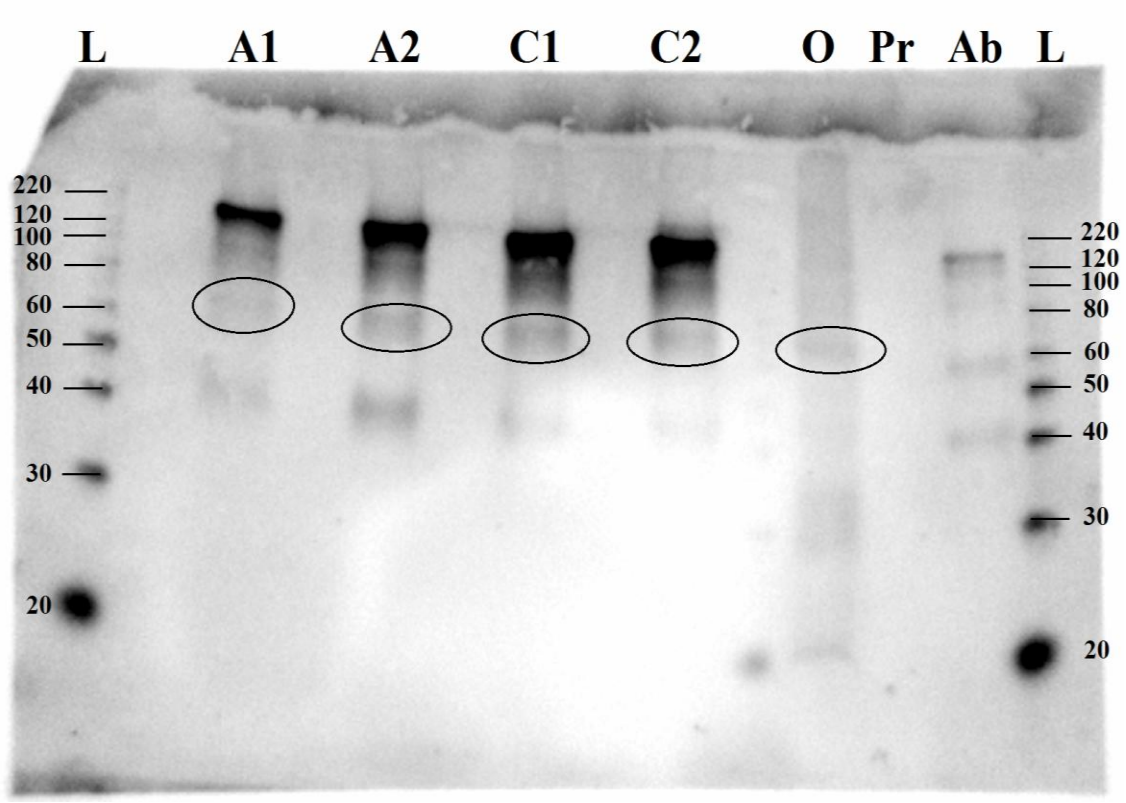

Figure 11 Western Blot Analysis of Anti-Cyclophilin B Co-immunoprecipitates from Endoplasmic Reticulum-Enriched Hepatocyte Lysates.

L: Protein standards. Values in kilodaltons (kD).
A1: HERDA homozygote 1, Anti-CYPB immunoprecipitate.
A2: HERDA homozygote 2, Anti-CYPB immunoprecipitate.
C1: Control 1, Anti-CYPB immunoprecipitate.
C2: Control 2, Anti-CYPB immunoprecipitate.
O: Mouse Ovarian Cell Lysate (LH1 positive control).
Pr: CYPB purified protein (CYPB positive control).
Ab: Anti-CYPB antibody.
Note (○) 85 kD bands in HERDA affected and control lanes.

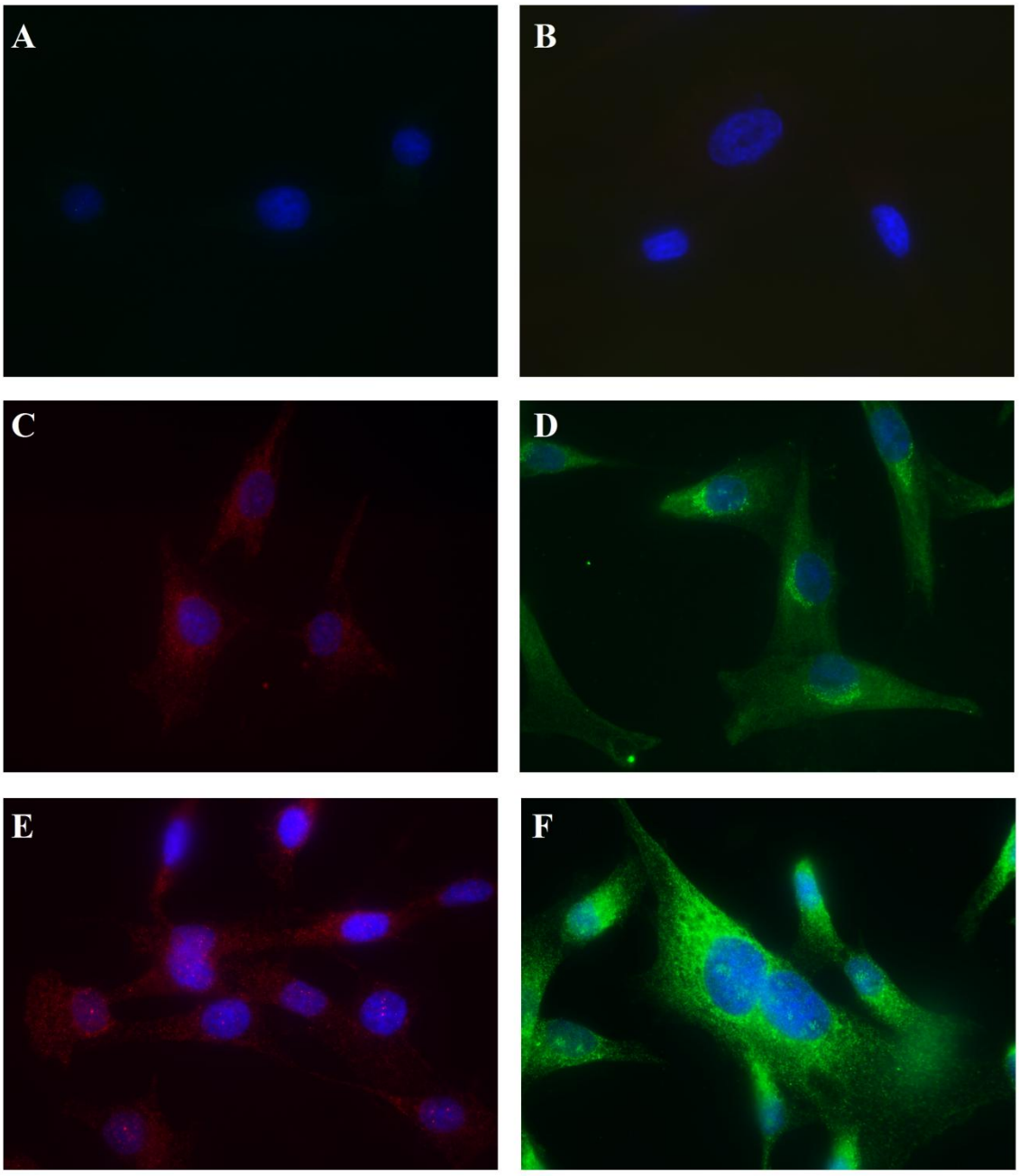

Figure 12 Immunofluorescence Assays using Control Fibroblasts.

A: Secondary antibody only, donkey anti-goat FITC (1:200).
B: Secondary antibody only, goat anti-rabbit TRED (1:400).
C: Standard immunofluorescence, primary anti-CYPB antibody (1:200).
D: Standard immunofluorescence, primary anti-LH1 antibody (1:200).
E: Standard immunofluorescence, primary anti-P3H1 antibody (1:600).
F: Standard immunofluorescence, primary anti-CRTAP antibody (1:200).

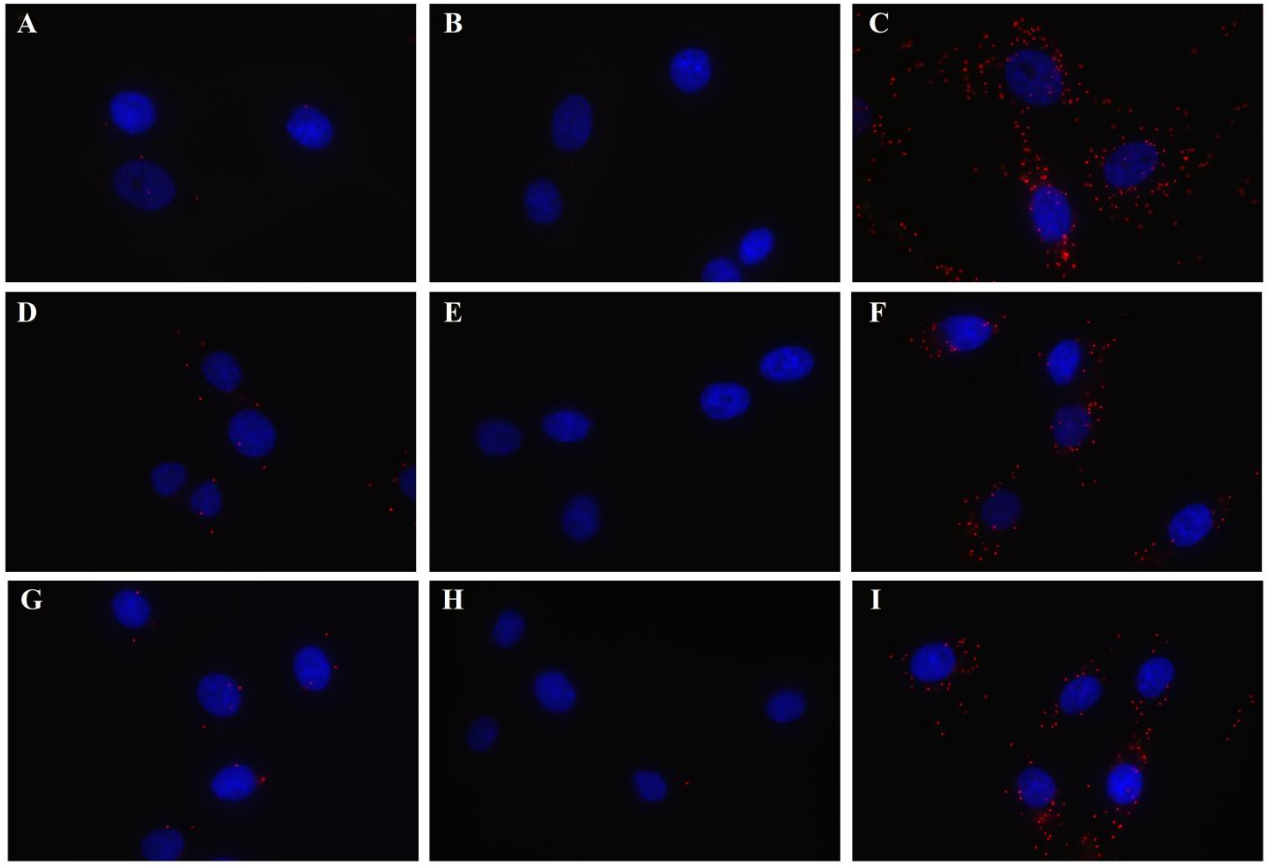

Figure 13 Duolink Proximity Ligation Assay (PLA) for CYPB and LH1 in Equine Fibroblasts.

A) HERDA negative, anti-CYPB only (1:100) **B**) HERDA negative, anti-LH1 only (1:100). **C**) HERDA negative, CYPB-LH1 PLA.
D) Heterozygote, anti-CYPB only (1:100). **E**) Heterozygote, anti-LH1 only (1:100). **F**) Heterozygote, CYPB-LH1 PLA.
G) Homozygote, anti-CYPB only (1:100). **H**) Homozygote, anti-LH1 only (1:100). **I**) Homozygote, CYPB-LH1 PLA.
NOTE: Single-antibody stains should not produce signal. Signal should only be present in cells stained with two antibodies.

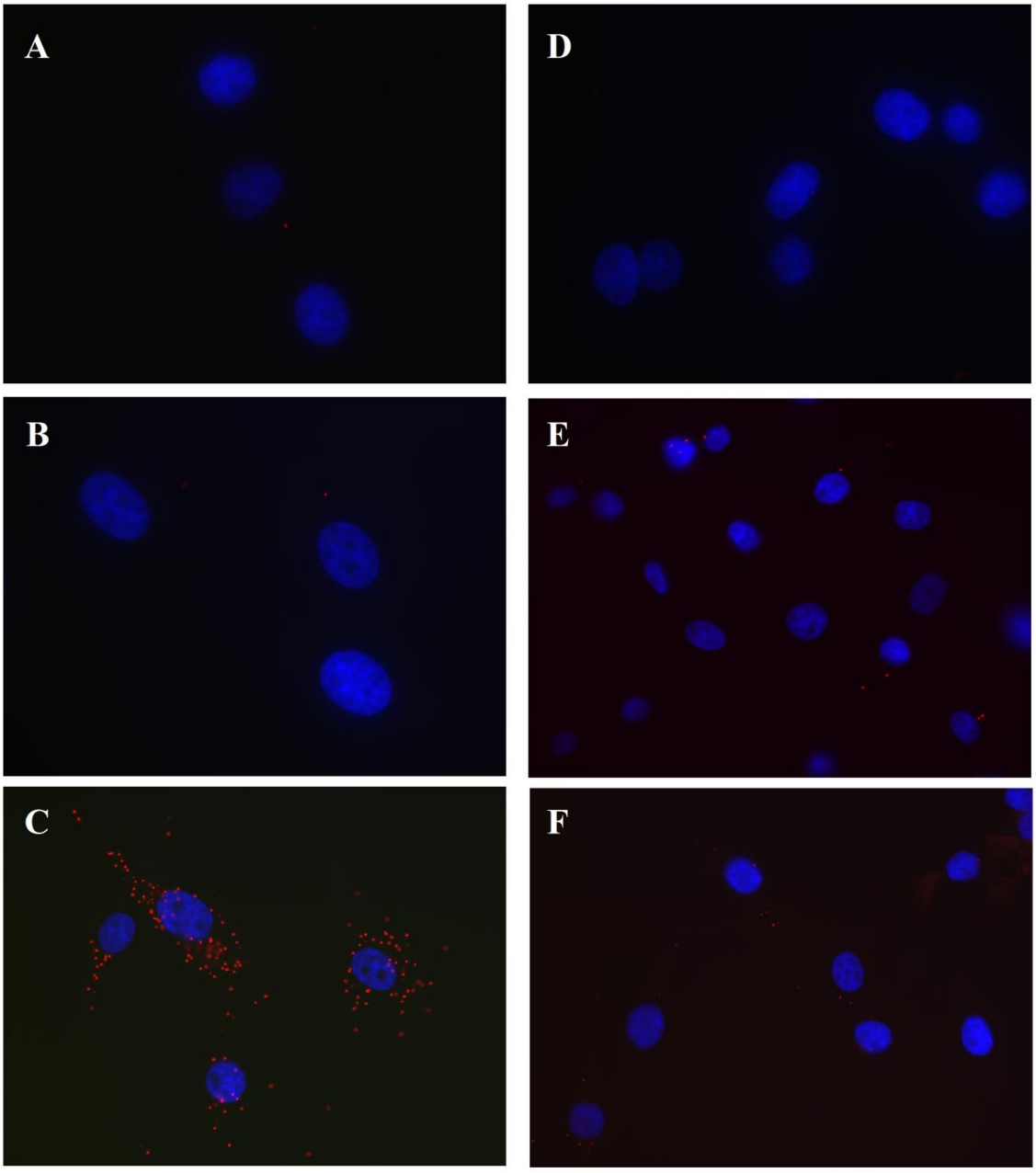

Figure 14 Duolink Proximity Ligation Assay (PLA) for CRTAP and P3H1 in Equine Fibroblasts.

A) HERDA negative, anti-CRTAP only (1:2000) **B**) HERDA negative, anti-P3H1 only (1:4000). **C**) HERDA negative, CRTAP-P3H1 PLA. **D**) Homozygote, anti-CRTAP only (1:2000). **E**) Homozygote, anti-P3H1 only (1:4000). **F**) Homozygote, CRTAP-P3H1 PLA.
NOTE: Single-antibody stains should not produce signal. Signal should only be present in cells stained with two antibodies.

CHAPTER V

CONCLUSION

In this project, we have designed and validated a low cost device for quantifying physical properties of connective tissue specimens with inherently high tensile strength. Results of testing performed on normal equine deep digital flexor tendon indicate that this device provides a practical method of adequately securing larger tendons and ligaments for tensile strength testing.

Using this method, we found that HERDA horses have significantly altered tensile properties of multiple tissues with high Type I fibrillar collagen content, substantiating that the molecular mutation associated with HERDA that alters collagen fibrillogenesis is not limited to the integument. In addition, these changes of reduced tensile strength and elastic modulus of energy-storing tissues have a strong positive correlation with improved locomotor efficiency of tendons and ligaments (Minetti, 1999; Souza, 2010; Thorpe, 2010, 2012).

Finally, we have provided substantiation that CYPB and LH1 interact within the endoplasmic reticulum of all fibroblasts. Furthermore, we found attenuation of this interaction in fibroblasts containing either one or both copies of the mutant HERDA PPIB allele and interactions between P3H1 and CRTAP also appear to be attenuated in cells homozygous for the HERDA mutation. This information helps to further clarify the

mechanistic link between the known HERDA PPIB mutation and the documented disease phenotype.

This discovery of evidence for a small but quantifiable HERDA phenotype in heterozygotes, along with documented changes in tensile properties of tendinoligamentous structures of homozygotes introduces the concept of heterozygote phenotypes in animal disease and provides a plausible hypothesis for causality between carrier status and athletic advantage.

REFERENCES

Abbas N, Lücking CB, Ricard S, Dürr A, Bonifati V, De Michele G, Bouley S, Vaughan JR, Gasser T, Marconi R, Broussolle E, Brefel-Courbon C, Harhangi BS, Oostra BA, Fabrizio E, Böhme GA, Pradier L, Wood NW, Filla A, Meco G, Denefle P, Agid Y, Brice A. A wide variety of mutations in the parkin gene are responsible for autosomal recessive parkinsonism in Europe. French Parkinson's Disease Genetics Study Group and the European Consortium on Genetic Susceptibility in Parkinson's Disease. Hum Mol Genet 1999;8:567-74.

Amiel D, Frank C, Harwood F, Fronek J, Akeson W. Tendons and Ligaments: A Morphological and Biochemical Comparison. J Orthopaed Res 1984;1:257-265.

Arlein MS. Generalized acute cutaneous asthenia in a dog. J Am Vet Med Assoc 1947;111:52.

Azadani AN, Chitsaz S, Matthews PB, Jaussaud N, Leung J, Wisneski A, Ge L, Tseng EE. Biomechanical comparison of human pulmonary and aortic roots. Eur J Cardiothorac Surg 2012;41:1111-1116.

Bachinger HP. The influence of peptidyl-prolyl cis-trans isomerase on the in vitro folding of Type III collagen. J Biol Chem 1987;262:17144-14148.

Barnes MJ. Collagen in atherosclerosis. Coll Relat Res 1985;5:65-97.

Barnes AM, Carter EM, Cabral WA, Weis MA, Chang W, Makareeva E, Leikin S, Rotimi CN, Eyre DR, Raggio CL, Marini JC. Lack of Cyclophilin B in Osteogenesis Imperfecta with Normal Collagen Folding. New Engl J Med 2010;362:521-528.

Beighton P, De Paepe A, Steinmann B, Tsipouras P, Wenstrup RJ. Ehlers-Danlos Syndromes: revised nosology, Villefranche, 1997. Am J Med Genet 1998;77:31-37.

Birch HL, Wilson AM, Goodship AE. Physical activity: does long-term high-intensity exercise in horses result in tendon degeneration? J Appl Physiol 2008;105:1927-1933.

Bishop JE, Guerreiro D, Laurent GJ. Changes in composition and metabolism of arterial collagens during the development of pulmonary hypertension in rabbits. Am Rev Resp Dis 1990;41:450-455.

Borges AS, Conceicão LG, Alves ALG, Fabris VE, Pessoa MA. Hereditary equine regional dermal asthenia in three related Quarter Horses in Brazil. Vet Dermatol 2005;16:125-130.

Bowser JE, Elder SH, Rashmir-Raven AM, Swiderski CE. A cryogenic clamping technique that facilitates ultimate tensile strength determinations in tendons and ligaments. Vet Comp Orthop Traumatol 2011;24:370-373.

Brounts SH, Rashmir-Raven AM, Black SS. Zonal dermal separation: a distinctive histopathological lesion associated with hyperelastosis cutis in a Quarter Horse. Vet Dermatol 2001;12:219-24.

Brown PJ, Young RD, Cripps PJ. Abnormalities of collagen fibrils in a rabbit with a connective tissue defect similar to Ehlers-Danlos syndrome. Res Vet Sci 1993; 55: 346-350.

Cabral WA, Chang W, Barnes AM, Weis MA, Scott MA, Leikin S, Makareeva E, Kuznetsova NV, Rosenbaum KN, Tifft CJ, Bulas DI, Kozma C, Smith PA, Eyre DR, Marini JC. Prolyl 3-hydroxylase 1 deficiency causes a recessive metabolic bone disorder resembling lethal/severe osteogenesis imperfect. Nature 2007; 39:359-365.

Canty EG, Kadler KE. Procollagen trafficking, processing and fibrillogenesis. J Cell Sci 2005;118:1341-1353.

Christiansen HE, Schwarze U, Pyott SM, AlSwaid A, Balwi MA, Alrasheed S, Pepin MG, Weis MA, Eyre DR, Byers PH. Homozygosity for a missense mutation in SERPINH1, which encodes the collagen chaperone protein HSP47, results in severe recessive Osteogenesis Imperfecta. Am J Hum Genet 2010;86:389-398.

Choi JW, Sutor SL, Lindquist L, Evans GL, Madden BJ, Bergen HR III, Hefferan TE, Yaszemski MJ, Bram RJ. Severe Osteogenesis Imperfecta in cyclophilin B deficient mice. PLoS Genet 2009;5:1-12.

Contino EK, Park RD, McIlwraith CW. Prevalence of radiographic changes in yearling and 2-year-old Quarter Horses intended for cutting. Equine Vet J 2012;44:185–195.

Crevier N, Porcelot P, Denoix JM, Geiger D, Bortolussi C, Ribot X, Sanaa M. Segmental variations of in vitro mechanical properties in equine superficial digital flexor tendons. Am J Vet Res 1996;57:1111-1117.

Dagda RK, Cherra SJ 3rd, Kulich SM, Tandon A, Park D, Chu CT. Loss of PINK1 function promotes mitophagy through effects on oxidative stress and mitochondrial fission. J Biol Chem 2009;284:13843-13855.

Davis JR. Tensile testing, 2nd Edition. In: Uniaxial Tensile Testing. Ed: J.R. Davis, ASM International, Materials Park, Ohio. 2004: 33-59.

Dombi GW, Haut RC, Sullivan WG. Correlation of high-speed tensile strength with collagen content in control and lathyritic rat skin. J Surg Res 1993;54:21-28.

Endrich MM, Gehrig P, Gehring H. Maturation- induced conformational changes of HIV-1 capsid protein and identification of two high affinity sites for cyclophilins in the C-terminal domain. J Biol Chem 1999;274:5326–5332.

Epstein EH Jr, Munderloh NH. Human skin collagen: Presence of Type I and Type III at all levels of the dermis. J Biol Chem 1978;253:1336-1337.

Fernandes NF, Schwartz RA. A "hyperextensive" review of Ehlers-Danlos syndrome. Cutis 2008;82:242-248.

Fratzel P. Collagen: Structure and mechanics, an introduction. In: Collagen structure and mechanics. Ed: P. Fratzl, Springer Science + Business Media, LLC, New York. 2008: 9-41.

Grady JG, Elder SH, Ryan PL, Swiderski CE, Rashmir-Raven AM. Biomechanical and molecular characteristics of hereditary equine regional dermal asthenia in Quarter Horses. Vet Dermatol 2009;20:591-599.

Gunson DE, Halliwell RE, Minor RR. Dermal collagen degradation and phagocytosis. Occurrence in a horse with hyperextensible fragile skin. Arch Dermatol 1984; 120:599-604.

Hardy MH, Fisher KR, Vrablic OE, Yager JA, Nimmo-Wilkie JS, Parker W, Keeley FW. An inherited connective tissue disease in the horse. Lab Invest 1988;59:253-262.

Harvey RG, Brown PJ, Young RD, Whitbread TJ. A connective tissue defect in two rabbits similar to Ehlers-Danlos syndrome. Vet Rec 1990;126:130-132.

Hedrich K, Hagenah J, Djarmati A, Hiller A, Lohnau T, Lasek K, Grünewald A, Hilker R, Steinlechner S, Boston H, Kock N, Schneider-Gold C, Kress W, Siebner H, Binkofski F, Lencer R, Münchau A, Klein C. Clinical spectrum of homozygous and heterozygous PINK1 mutations in a large German family with Parkinson disease: role of a single hit? Arch Neurol 2006;63:833-838.

Hill A. (2010). *Skin from horses with hereditary equine regional dermal asthenia (HERDA) contains collagen crosslinking patterns that are associated with reduced tensile strength [electronic resource] / by Ashley Arwen Hill*. Mississippi State : Mississippi State University, 2010.

Holbrook KA, Byers PH, Counts DF, Hegreberg GA. Dermatosparaxis in a Himalayan cat. II. Ultrastructural studies of dermal collagen. J Invest Dermatol 1980;74:100-104.

Horibe T, Yosho C, Okada S, Tsukamoto M, Nagai H, Hagiwara Y, Tujimoto Y, Kikuchi M. The chaperone activity of protein disulfide isomerase is affected by cyclophilin B and cyclosporin A in vitro. J Biochem 2002;132:401–407.

Hosoda Y, Kawano K, Yamasawa F, Ishii T, Shibata T, Inayama S. Age-dependent changes of collagen and elastin content in human aorta and pulmonary artery. Angiology 1984;35:615-621.

http://equistat.com/

Ishikawa Y, Wirz J, Vranka JA, Nagata K, Bachinger HP. Biochemical characterization of the prolyl 3-hydroxylase 1. cartilage associated protein. cyclophilin B complex. J Biol Chem 2009;284:17641-17647.

Ishikawa Y, Vranka JA, Boudko SP, Pokidysheva E, Mizuno K, Zientek K, Keene DR, Rashmir-Raven AM, Nagata K, Winand NJ, Bachinger HP. The mutation in cyclophilin B that causes hyperelastosis cutis in the American Quarter Horse does not affect peptidyl-prolyl cis-trans isomerase activity, but shows altered cyclophilin B-protein interactions and affects collagen folding. J Biol Chem 2012; 287:22253-22265.

Jansen MO, Savelberg HHCM. Stress and strain of equine tendons of the forelimb at failure. Equine Vet J 1994;S17:57-60.

Jopp I, Reese S. Morphological and biomechanical studies on the common calcaneal tendon in dogs. Vet Comp Orthop Tramatol 2009;22:119-124.

Khan NL, Scherfler C, Graham E, Bhatia KP, Quinn N, Lees AJ, Brooks DJ, Wood NW, Piccini P. Dopaminergic dysfunction in unrelated, asymptomatic carriers of a single parkin mutation. Neurology 2005;64:134-136.

King JD, Bobechko WP. Osteogenesis Imperfecta: An orthopaedic description and surgical review. J Bone Joint Surg 1971;53B(1):72-89.

Kozlov G, Bastos-Aristizabal S, Maattanen SP, Rosenauer A, Zheng F, Killikelly A, Trempe JF, Thomas DY, Gehring K. Structural basis of cyclophilin B binding by the calnexin/calreticulin P-domain. J Biol Chem 2010;285:35551–35557.

Krane SM. The importance of proline residues in the structure, stability and susceptibility to proteolytic degradation of collagens. Amino Acids 2008;35:703-710.

Lee S. Cornell researchers develop DNA test to identify debilitating equine skin disease. J Equine Vet Sci 2008;28:57.

Lerner DJ, McCracken MD. Hyperelastosis cutis in two horses. J Am Anim Hosp Ass 1978;2:350-352.

Liu J, Albers MW, Chen CM, Schreiber SL, Walsh CT. Cloning, expression, and purification of human cyclophilin in Escherichia coli and assessment of the catalytic role of cysteines by site-directed mutagenesis. Proceedings of the National Academy of Sciences USA 1990;87:2304-2308.

Lodish HF, Kong N. Cyclosporin A inhibits an initial step in folding of transferrin within the endoplasmic reticulum. J Biol Chem 1991;266:14835–14838.

Lovell CR, Smolenski KA, Duance VC, Light ND, Young S, Dyson M. Type I and III collagen content and fibre distribution in normal human skin during ageing. Br J Dermatol 1987;117:419-428.

Marini JC, Cabral WA, Barnes AM, Chang W. Components of the collagen proyly 3-hydroxylation complex are crucial for normal bone development. Cell Cycle 2007;6:1675-1681.

Mao JR, Bristow J. The Ehlers-Danlos syndrome: on beyond collagens. J Clin Invest 2001;107:1063–1069.

Meunier L, Usherwood YK, Chung KT, Hendershot LM. A subset of chaperones and folding enzymes form multiprotein complexes in endoplasmic reticulum to bind nascent proteins. Mol Biol Cell 2002;13:4456–4469.

Miller EJ. Biochemical characteristics and biological significance of the genetically-distinct collagens. Molec Cell Biochem 1976;13:165-192.

Minetti AE, Ardigo LP, Reinach E, Saibene F. The relationship between mechanical work and energy expenditure of locomotion in horses. J Exp Biol 1999;202:2329–2338.

Minor RR, Lein DH, Patterson DF, Krook L, Porter TG, Kane AC. Defects in collagen fibrillogenesis causing hyperextensible, fragile skin in dogs. J Am Vet Med Ass 1983;182:142-148.

Mochal CA, Miller WW, Cooley AJ, Linford RL, Ryan PL, Rashmir-Raven AM. Ocular findings in Quarter Horses with hereditary equine regional dermal asthenia. J Am Vet Med Ass 2010;237:304-310.

Myllylä R, Pajunen L, Kivirikko KI. Polyclonal and monoclonal antibodies to human lysyl hydroxylase and studies on the molecular heterogeneity of the enzyme. Biochem J 1988;253:489-496.

Pasquali M, Dembure PP, Still MJ, Elsas LJ. Urinary pyridinium cross-links: A noninvasive diagnostic test for Ehlers-Danlos syndrome type VI. New Eng J Med 1994;331:132-133.

Pasquali M, Still MJ, Vales T, Rosen RI, Evinger JD, Dembure PP, Longo N, Elsas LJ. Abnormal formation of collagen cross-links in skin fibroblasts cultured from patients with Ehlers-Danlos syndrome type VI. Proc Assoc Am Physicians 1997;109:33-41.

Ploeg M, Saey V, de Bruijn CM, Gröne A, Chiers K, van Loon G, Ducatelle R, van Weeren PR, Back W, Delesalle C. Aortic rupture and aorto-pulmonary fistulation in the Friesian horse: Characterisation of the clinical and gross post mortem findings in 24 cases. Equine Vet J 2012 In Press: doi: 10.1111/j.2042-3306.2012.00580.x.

Pousi B, Hautala T, Hyland JC, Schröter J, Eckes B, Kivirikko KI, Myllylä R. A compound heterozygote patient with Ehlers-Danlos syndrome type VI has a deletion in one allele and a splicing defect in the other allele of the lysyl hydroxylase gene. Hum Mutat 1998;11:55-61.

Pyott SM, Schwarze U, Christiansen HE, Pepin MG, Leistritz DF, Dineen R, Harris C, Burton BK, Angle B, Kim K, Sussman MD, Weis MA, Eyre DR, Russell DW, McCarthy KJ, Steiner RD, Byers PH. Mutations in PPIB (cyclophilin B) delay Type I procollagen chain association and result in perinatal lethal to moderate osteogenesis imperfecta phenotypes. Hum Mol Genet 2011;20:1595-1609.

Rashmir-Raven AM, Winand NJ, Read RW, Hopper RM, RyanPL, Poole MH, Erb HN. (2004) Equine hyperelastosis cutis update. In: Proceedings of the 50th Annual American Association of Equine Practitioners Convention, Denver, CO. pp 47-50.

Rendle DI, Durham AE, Smith KC. Hereditary equine regional dermal asthenia in a Quarter Horse bred in the United Kingdom. Vet Rec 2008;162:20-22.

Riemersma DJ, Schamhardt HC. The cryo-jaw, a clamp designed for in vitro rheology studies of horse digital flexor tendons. J Biomech 1982;15:619-620.

Rincón L, Schatzmann L, Brunner P, Stäubli HU, Ferguson SJ, Oxland TR, Nolte L-P. Design and evaluation of a cryogenic soft tissue fixation device- load tolerances and thermal aspects. J Biomech 2001;34:393-397.

Sambrook J, Russell DW. Molecular cloning: a laboratory manual.3rd Edition Ed: J. Sambrook, Cold Spring Harbor Laboratory Press, Cold Spring Harbor, New York. 2001 pp 18.1-18.6.

Sequeira JL, Rocha NS, Bandarra EP, Figueiredo LMA, Eugenio FR. Collagen dysplasia (Cutaneous Asthenia) in a cat. Vet Pathol 1999;36:603-606.

Smith RKW. Physiology of Tendon and Ligament. 9th Congress on Equine Medicine & Surgery. Geneva, Switzerland. Ithaca: International Veterinary Information Service (www.ivis.org), 2005; Document No. P1903.1205.

Smith T, Ferreira LR, Herbert C, Norris K, Sauk JJ. Hsp47 and cyclophilin B traverse the endoplasmic reticulum with procollagen into pre-Golgi intermediate vesicles. A role of Hsp47 and cyclophilin B in the export of procollagen from the endoplasmic reticulum. J Biol Chem 1995;270:18323-18328

Solomons B. Equine cutis hyperelastica. Equine Vet J 1984;16:541-542.

Soslowsky LJ, Thomopoulos S, Esmail A, Flanagan CL, Iannotti JP, Williamson JD III, Carpenter JP. Rotator cuff tendonitis in an animal model: role of extrinsic and overuse factors. Ann Biomed Eng 2002;30:1057-1063.

Souza MV, van Weeren PR, van Schie HTM, van de Lest CHA Regional differences in biochemical, biomechanical, and histomorphological characteristics of the equine suspensory ligament. Equine Vet J 2010;42:611-620.

Stannard AA. Congenital diseases. Vet Dermatol 2000;11:211-215.

Steinmann B, Bruckner P, Superti-Furga A. Cyclosporin A slows collagen triple-helix formation in vivo: indirect evidence for a physiologic role of peptidyl-prolyl cis–trans-isomerase. J Biol Chem 1991;266:1299–1303.

Swiderski C, Pasquali M, Schwarz L, Boyle C, Read R, Hopper R, Ryan P, Rashmir-Raven R. The ratio of urine deoxypyridinoline to pyridinoline identifies horses with hyperelastosis cutis (A.K.A. hereditary equine regional dermal asthenia or HERDA). Proceedings of the American College of Veterinary Internal Medicine 2006; 163:756.

Swiderski CE, Rashmir-Raven AM, Pasquali M, inventors; University of Utah Research Foundation, assignee. Diagnosing equine hyperelastosis cutis. United States patent US 20070105234A1. 2007 May 10.

Tajima M, Miyake S, Takehana K, Kobayashi A, Yamato O, Maede Y. Gene defect of dermatan sulfate proteoglycan of cattle affected with a variant form of Ehlers-Danlos syndrome. J Vet Intern Med 1999;13:202-205.

Tan LC, Tanner CM, Chen R, Chan P, Farrer M, Hardy J, Langston JW. Marked variation in clinical presentation and age of onset in a family with a heterozygous parkin mutation. Mov Disord 2003;18:758-763.

Thorpe CT, Stark RJF, Goodship AE, Birch HL. Mechanical properties of the equine superficial digital flexor tendon relate to specific collagen cross-link levels. Equine Vet J 2010;42:538-543.

Thorpe CT, Udeze CP, Birch HL, Clegg PD, Screen HRC. Specialization of tendon mechanical properties results from interfascicular differences. J R Soc Interface 2012;9:3108-3117.

Tipton SG, Anderson JD, Smith TS, Linford R, Rashmir-Raven AM. Epidemiologic and economic study of hyperelastosis cutis/HERDA in the Quarter Horse cutting industry. J Anim Sci E-Supp 2008;86:516-558.

Trudel G, Doherty GP, Koike Y, Ramachandran N, Lecompte M, Dinh L, Uhthoff HK. Restoration of strength despite low stress and abnormal imaging after achilles injury. Med Sci Sports Exerc 2009;41:2009-2016.

Tryon RC, White SD, Famula TR, Schultheiss PC, Hamer DW, Bannasch DL. Inheritance of hereditary equine regional dermal asthenia in Quarter Horses. Am J Vet Res 2005;66:437-442.

Tryon RC, White SD, Bannasch DL. Homozygosity mapping approach identifies a missense mutation in equine cyclophilin B (PPIB) associated with HERDA in American Quarter Horses. Genomics. 2007;90:93-102.

Tryon RC, Penedo MCT, McCue ME, Valberg SJ, Mickelson JR, Famula TR, Wagner ML, Jackson M, Hamilton MJ, Nooteboom S, Bannasch DL. Evaluation of allele frequencies of inherited disease genes in subgroups of American Quarter Horses. J Am Vet Med Ass 2009;234:120-125.

Uzawa K, Yeowell HN, Yamamoto K, Mochida Y, Tanzawa H, Yamauchi M. Lysine hydroxylation of collagen in a fibroblast cell culture system. Biochem Biophys Res Commun 2003;305:484-7.

Valente EM, Salvi S, Ialongo T, Marongiu R, Elia AE, Caputo V, Romito L, Albanese A, Dallapiccola B, Bentivoglio AR. PINK1 mutations are associated with sporadic early-onset parkinsonism. Ana Neurology 2004;56:336-341.

Valtavaara M, Papponen H, Pirttila A-M, Hiltunen K, Helander H, Myllylä R. Cloning and characterization of a novel human lysyl hydroxylase isoform highly expressed in pancreas and muscle. J Biol Chem 1997;272:6831-6834.

van Dik FS, Nesbitt IM, Zwikstra EH, Nikkels PGJ, Piersma SR, Fratantoni SA, Jimenez CR, Huizer M, Morsman AC, Cobben JM, van Roij MHH, Elting MW, Verbeke JIML, Wijnaendts LCD, Shaw NJ, Hogler W, McKeown C, Sistermans EA, Dalton A, Meijers-Heijboer H, Pals G. PPIB Mutations cause severe Osteogenesis Imperfecta. Am J Hum Genet 2009;85:521-527.

van Halderen A, Green JR. Dermatosparaxis in white dorper sheep. J South Afr Vet Assoc 1988;59:45.

Vranka JA, Pokidysheva E, Hayashi L, Zientek K, Mizuno K, Ishikawa Y, Maddox K, Tufa S, Keene D, Klein R, Bachinger HP. Prolyl 3-hydroxylase 1 mice display abnormalities in fibrillar collagen-rich tissues such as tendons, skin, and bones. J Biol Chem 2010;285:17253-17262.

Walker LC, Teebi AS, Marini JC, De Paepe A, Atsawasuwan P, Yamauchi M, Yeowell HN. Decreased expression of lysyl hydroxylase 2 (LH2) in skin fibroblasts from three Ehlers-Danlos patients does not result from mutations in either the coding or proximal promoter region of the LH2 gene. Mol Genet Metab 2004;83:312-321.

White SD, Affolter VK, Bannasch DL, Schultheiss PC, Hamar DW, Chapman PL, Naydan D, Spier SJ, Rosychuk RAW, Rees C, Veneklasen GO, Martin A, Bevier D, Jackson HA, Bettenay S, Matousek J, Campbell KL, Ihrke PJ. Hereditary equine regional dermal asthenia ('hyperelastosis cutis') in 50 horses: clinical, histological, immunohistological and ultrastructural findings. Vet Dermatol 2004;15: 207-217.

White SD, Affolter VK, Schulteiss PC, Ball BA, Wessel MT, Kass P, Molinaro AM, Bannasch DL, Ihrke PJ. Clinical and pathological findings in a HERDA-affected foal for 1.5 years of life. Vet Dermatol 2007;18:36-40.

Wilhelm MT, Rufini A, Wetzel MK, Tsuchihara K, Inoue S, Tomasini R, Itie-Youten A, Wakeham A, Arsenian-Henriksson M, Melino G, Kaplan DR, Miller FD, Mak TW. Isoform-specific p73 knockout mice reveal a novel role for ΔNp73 in the DNA damage response pathway. Genes Dev 2010;24, 549-560.

Willing MC, Cohn DH, Starman B, Holbrook KA, Greenberg CR, Byers PH. Heterozygosity for a large deletion in the α2(I) collagen gene has a dramatic effect on Type I collagen secretion and produces perimatal lethal osteogenesis imperfect. J Biol Chem 1988;263:8398-8408.

Yeowell HN, Walker LC. Mutations in the lysyl hydroxylase 1 gene that result in enzyme deficiency and the clinical phenotype of Ehlers-Danlos syndrome type VI. Mol Genet Metab 2000;71:212-224.

Zhang Y, Gao J, Chung KK, Huang H, Dawson VL, Dawson TM. Parkin functions as an E2-dependent ubiquitin- protein ligase and promotes the degradation of the synaptic vesicle-associated protein, CDCrel-1. Proc Natl Acad Sci USA 2000;97:13354-13359.

Zhang J, Herscovitz H. Nascent lipidated apolipoprotein B is transported to the Golgi as an incompletely folded intermediate as probed by its association with network of endoplasmic reticulum molecular chaperones, GRP94, ERp72, BiP, calreticulin, and cyclophilin B. J Biol Chem 2003;278:7459–7468.

APPENDIX A

MANUFACTURERS' ADDRESSES

[a]MTS Systems Corporation, Eden Prairie, MN, USA.

[b]Test Resources, Inc., Shakopee, MN, USA.

[c]Biosyntech, Inc., Laval, Quebec, Canada.

[d]Ithaca, NY, USA.

[e]Nasco, 901 Janesville Avenue Fort Atkinson, WI, USA.

[f]Instron, Inc., Norwood, Massachusetts, USA.

[g]SAS Institute, Inc., Cary, NC, USA.

[h]Veterinary Genetics Laboratory, Old Davis Road, Davis, CA, USA.

[i]Sigma-Aldrich, 3506 South Broadway, St. Louis, MO, USA.

[j]Gemini Bio-Products, 930 Riverside Parkway, West Sacramento, CA, USA.

[k]Athena Enzyme Systems, 1450 South Rolling Rd. Baltimore. MD, USA.

[l]Thermo Scientific, 81 Wyman Street, Waltham, MA 02454 USA.

[m]Invitrogen, 1600 Faraday Avenue, PO Box 6482, Carlsbad, CA, USA.

[n]Santa Cruz Biotechnology, Inc., 2145 Delaware Avenue Santa Cruz, CA, USA.

[o]Bio-Rad Laboratories, 1000 Alfred Nobel Drive, Hercules, CA, USA.

[p]ProSpec-Tany TechnoGene Ltd. Ness Ziona, PO Box 4157 74140 Israel.

[q]Abcam, Inc., One Kendall Square, Bldg. 200, 3rd Floor, Cambridge, MA, USA.

[r]Pierce Protein Biology Products, 3747 N Meridian Rd, Rockford, IL, USA.

[s]Irvine Scientific, 2511 Daimler Street Santa Ana, CA, USA.

[t]Zymed Laboratories, Invitrogen, 458 Carlton Court S. San Francisco, CA, USA.

[u]Olink Bioscience, Dag Hammarskjölds väg 52 B752 37 Uppsala, Sweden.

[v]A gift to Dr Pyott from Roy Morello, Ph.D., Department of Physiology & Biophysics, University of Arkansas for Medical Sciences, 4301 W. Markham St., #505, Little Rock, AR, USA.

[w]Abnova Corperation, PO Box 1697, Walnut, CA, USA.

[x]Jackson Laboratories, 600 Main Street, Box 14, Bar Harbor, ME, USA.

[y]Molecular Probes, 29851 Willow Creek Road, Eugene, OR, USA.

[z]Nikon Instruments, Inc., 1300 Whitman Road, Melville, NY, USA.

[aa]Photometrics, Inc., 15801 Graham St, Huntington Beach, CA, USA.